

---

**Characterization of *AtST4c* function  
in flowering in *Arabidopsis thaliana***

Yao Zhang

A Thesis

In

The Department

Of

Biology

Presented in Partial Fulfillment of the Requirements

for the Degree of Master of Science at

Concordia University

Montreal, Quebec, Canada

January 2013

© Yao Zhang, 2013

CONCORDIA UNIVERSITY

School of Graduate Studies

This is to certify that the thesis prepared

By: **Yao Zhang**

Entitled: **Characterization of the function of *AtST4c* in flowering in *Arabidopsis thaliana***

and submitted in partial fulfillment of the requirements for the degree of

**Master of Science**

complies with the regulations of the University and meets the accepted standards with respect to originality and quality.

Signed by the final Examining Committee:

\_\_\_\_\_

Selvadurai Dayanandan

Chair

\_\_\_\_\_

Madoka Gray-Mitsumune

Examiner

\_\_\_\_\_

Paul Joyce

Examiner

\_\_\_\_\_

William Zerges

Examiner

\_\_\_\_\_

Luc Varin

Supervisor

Approved by

\_\_\_\_\_

Chair of Department or Graduate Program Director

\_\_\_\_\_

\_\_\_\_\_

Dean of Faculty

# ABSTRACT

## Characterization *AtST4c* function in flowering in *Arabidopsis thaliana*

Yao Zhang

Concordia University, 2013

A main interest of our laboratory is to characterize the function of the 17 sulfotransferase-coding genes of *Arabidopsis thaliana*. The purpose of my project is to elucidate the biochemical and biological functions of *AtST4c*, a member of the *AtST4* subfamily (*AtST4a*, *b* and *c*). *AtST4c* knockout plants were found to exhibit a photoperiod-independent early flowering phenotype suggesting that *AtST4c* plays a negative role in flowering induction. In addition, *AtST4c* knockout plants produced shorter primary roots, a reduced number of lateral roots, slightly smaller rosettes, fewer seeds per silique and finally smaller seeds, suggesting that *AtST4c* plays a positive role in *Arabidopsis* growth. Transcript expression studies showed that *AtST4c* is mainly expressed in roots and is repressed by the cytokinin *trans*-zeatin suggesting that the positive effect of *AtST4c* on plant growth is repressed by the cytokinin signaling pathway in *Arabidopsis*.

In order to further characterize the role of *AtST4c* in the control of flowering time, the expression of floral integrator genes such as *LEAFY*, *SUPPRESSOR OF*

*OVEREXPRESSION OF CO 1(SOC1)* and *APETALA 1* was studied in *AtST4c* mutant plants. Our results show up-regulation of *LEAFY* and *APETALA 1* in the mutant plants suggesting that *AtST4c* acts upstream of these two important meristem identity genes. However, no changes in *SUPPRESSOR OF OVEREXPRESSION OF CO 1(SOC1)* expression were observed suggesting that the early flowering phenotype is independent of four of the five pathways that promote flowering in Arabidopsis. Taken together our results suggest that *AtST4c* participates in the control of flowering time via the aging pathway or by interfering with the repression mediated by the gene *TERMINAL FLOWER 1*.

To characterize the biochemical function of *AtST4c*, we compared the sulfated metabolome of *AtST4c* knockout mutant plants and wild-type plants using liquid chromatography-mass spectrometry. Using this approach we were able to propose a structure for the substrate of *AtST4c*.

## Table of contents

ABSTRACT.....	ii
List of figures.....	vii
List of Tables.....	ix
List of abbreviations .....	x
Chapter 1- Introduction.....	- 1 -
1.1 Sulfotransferases .....	- 1 -
1.2 <i>AtST4</i> subfamily.....	- 4 -
1.3 Regulation of flowering time in <i>Arabidopsis thaliana</i> .....	- 7 -
1.4 Purpose of the present studies.....	- 14 -
Chapter 2- Materials and Methods.....	- 16 -
2.1 Materials .....	- 16 -
2.2 Methods.....	- 16 -
Plant growth conditions .....	- 16 -
Seed sterilization.....	- 17 -
Validation of the <i>AtST4c</i> T-DNA insertion knockout lines .....	- 17 -
Phenotype analysis of <i>AtST4c</i> -knockout plants .....	- 18 -
Expression, purification and <i>in vitro</i> assays of the <i>AtST4c</i> recombinant enzyme .....	- 19 -
Transcript expression study of <i>AtST4c</i> in response to cytokinins.....	- 20 -
Quantitative RT-PCR .....	- 21 -
Mass spectrometry .....	- 22 -
Chapter 3- Results.....	- 24 -
3.1 Introduction.....	- 24 -
3.2 Characterization of <i>AtST4c</i> biological function.....	- 25 -
3.2.2 Identification of homozygous <i>AtST4ac</i> T-DNA insertion line.....	- 25 -
3.2.3 Phenotype of the Arabidopsis <i>AtST4ac</i> double mutant line.....	- 27 -
3.3 Biochemical characterization of <i>AtST4c</i> .....	- 30 -

3.3.1 Introduction.....	- 30 -
3.3.2 Expression and assay of the AtST4c recombinant enzyme .....	- 30 -
3.3.3 HPLC purification of the substrate and enzymatic reaction product of AtST4c .....	- 31 -
3.3.4 Neutral loss mass spectrometry of the AtST4c purified product....	- 36 -
3.3.5 LC-MS/MS analysis of the AtST4c purified product .....	- 33 -
3.4 Regulation of <i>AtST4c</i> expression.....	- 40 -
3.4.1 <i>AtST4a</i> and <i>AtST4c</i> expression in different tissues of wild type Arabidopsis at different development stages. ....	- 40 -
3.4.2 Transcript expression study <i>AtST4c</i> in response to cytokinins .....	- 42 -
3.4.3 <i>AtST4c</i> expression in wild type and <i>lfy</i> mutant plants. ....	- 44 -
3.4.4 Expression profile of genes regulating flowering time in the AtST4c knockout mutant.....	- 48 -
Chapter 4- Discussion.....	- 51 -
References.....	- 60 -

## List of figures

Figure 1. Phylogenetic tree of <i>Arabidopsis thaliana</i> sulfotransferases .....	- 4 -
Figure 2. Flowering phenotype of wild-type <i>Arabidopsis thaliana</i> and knockout lines .....	- 7 -
Figure 3. Integration of the flowering time pathways.....	- 12 -
Figure 4. Characterization of the <i>AtST4ac</i> double mutant line.....	- 26 -
Figure 5. Flowering phenotype of <i>Arabidopsis thaliana</i> wild-type and knockout lines.....	- 28 -
Figure 6. Early flowering phenotype of <i>AtST4ac</i> double knockout plants.....	- 28 -
Figure 7. Reproductive developments of <i>AtST4ac</i> double knockout plants.....	- 29 -
Figure 8. SDS-PAGE of purified AtST4c recombinant enzyme.....	- 31 -
Figure 9. Enzymatic activity profile of the HPLC fractionated acid hydrolyzed root extract.....	- 35 -
Figure 10. HPLC purification of the AtST4c radiolabeled enzymatic product.....	- 36 -
Figure 11. Mass spectrometry of wild-type and <i>AtST4ac</i> double knockout crude root extracts.....	- 37 -
Figure 12. Chromatogram of the ion with a m/z of 498 [M+H] from wild-type and <i>AtST4ac</i> double knockout root extracts. ....	- 38 -

Figure 13.LC-MS/MS spectrum of the AtST4c sulfated product in negative mode.  
..... - 39 -

Figure 14. Expression profiles of AtST4a and AtST4c in aerial parts and roots of  
Arabidopsis at different developmental stages.. ..... - 41 -

Figure 15.Quantitative RT-PCR profiles of *AtST4* subfamily members in response  
to cytokinins..... - 43 -

Figure 16. Relative expression of *LEAFY* and *AtST4c* in wild-type Arabidopsis  
plants..... - 47 -

Figure 17. Relative expression levels of *AtST4c* in wild type and *lfy* mutant of  
Arabidopsis as determined by quantitative RT-PCR..... - 50 -

Figure 18 (a). Relative expression patterns of the flowering genes *LEAFY* and  
*APETALA1* in *AtST4c* knockout plants grown under long day  
condition.....- 50 -

Figure 18 (b). Relative expression patterns of the flowering genes *APETALA2*  
and *SOCI* in *AtST4c* knockout plants grown under long day  
condition.....- 51-

## List of Table

Table 1. Some of the important floral integrator genes of <i>Arabidopsis thaliana</i> .....	12
---	----

## List of abbreviations

<b><i>AGL24</i></b>	<i>AGAMOUS LIKE 24</i>
<b>AtST</b>	<i>Arabidopsis thaliana</i> sulfotransferase
<b><i>API</i></b>	<i>APETALA1</i>
<b><i>AP2</i></b>	<i>APETALA2</i>
<b>BLAST</b>	Basic local alignment search tool
<b>cDNA</b>	Complementary deoxyribonucleic acid
<b>CKs</b>	Cytokinins
<b><i>CO</i></b>	Constants gene
<b>Col-0</b>	Columbia 0
<b>Da</b>	Dalton
<b>DMSO</b>	Dimethyl sulfoxide
<b>DNA</b>	Deoxyribonucleic acid
<b>dNTP</b>	Deoxynucleotide triphosphates
<b>DTT</b>	DL-Dithiothreitol
<b><i>E.coli</i></b>	<i>Escherichia coli</i>
<b><i>FLC</i></b>	<i>FLOWERING LOCUS C</i>
<b><i>FT</i></b>	<i>FLOWERING LOCUS T</i>
<b>GA</b>	Gibberellic acid
<b>His-tag</b>	Histidine-tag

<b>HPLC</b>	High performance liquid chromatography
<b>IAA</b>	Indole-3-acetic acid
<b>IPTG</b>	Isopropyl $\beta$ -D thioglucoside
<b>LC-MS/MS</b>	Reverse phase liquid chromatography-tandem mass spectrometry
<b>LD</b>	Long day photoperiod
<b><i>LFY</i></b>	<i>LEAFY</i>
<b>MES</b>	2-Morpholino Ethane Sulfonic acid
<b>MS</b>	Mass spectroscopy
<b>MS medium</b>	Murashige and Skoog medium
<b>N-terminus</b>	Amino-terminus
<b>PAGE</b>	Polyacrylamide gel electrophoresis
<b>PAP</b>	3'-phosphoadenosine 5'-phosphate
<b>PAPS</b>	3'-phosphoadenosine 5'-phosphosulfate
<b>RNA</b>	Ribonucleic acid
<b>RT-PCR</b>	Reverse transcription polymerase chain reaction
<b>SD</b>	Short day condition
<b>SDS</b>	Sodium dodecyl sulfate
<b><i>SOCI</i></b>	<i>SUPPRESSOR OF OVEREXPRESSION OF CO 1</i>
<b>SPL</b>	<i>SQUAMOSA PROMOTER BINDING PROTEIN-LIKE</i>
<b>SULT</b>	Sulfotransferase

<b><i>SVP</i></b>	<i>SHORT VEGETATIVE PHASE</i>
<b>T-DNA</b>	Transferred-deoxyribonucleic acid fragment
<b>TLC</b>	Thin layer chromatography
<b>Tris</b>	Tris-[hydroxymethyl] aminomethane
<b><i>t-Zeatin</i></b>	<i>Trans-zeatin</i>

# Chapter 1- Introduction

## 1.1 Sulfotransferases

Sulfotransferases (SULTs) are enzymes which catalyze the transfer of a sulfonyl group ( $\text{SO}_3^-$ ) from the universal donor 3'-phosphoadenosine 5'-phosphosulphate (PAPS) to the hydroxyl group of the substrate with the parallel formation of 3'-phosphoadenosine 5'-phosphate (PAP).

Members of the SULT super-family can be found in most organisms from bacteria to mammals. Their substrates and functions vary considerably from one organism to another (Baek et al., 2010). The sulfonation reaction can either activate or inactivate the biological response that is normally mediated by the substrate. SULTs have been shown to play crucial roles in cell growth, development and defense (Baek et al., 2010). SULTs have highly conserved domains and structural similarities, and based on their affinity for different classes of substrates, they can be classified into two main groups. One group is membrane-associated and accepts macromolecular substrates, such as proteins, peptides and glycosaminoglycans (Niehrs et al., 1994). The second group comprises soluble proteins which sulfonate small organic molecules, such as flavonoids, steroids and xenobiotics.

Mammalian SULTs catalyse the conjugation of many neurotransmitters and steroid hormones (Klein and Papenbrock, 2004). In addition, mammalian cytosolic SULTs play an important role in the phase II of the biotransformation and excretion of

xenobiotics in the liver (Yasuda et al., 2005). The sulfonation reaction can be considered as a mechanism to protect cells against toxic chemicals (Negishi et al., 2001).

In the past 10 years, we have started to accumulate a lot of information about the biochemical functions of SULTs in plants (reviewed by Marsolais et al., 2007 ). However, the elucidation of their biological functions has proven difficult. The plant SULTs catalyze the sulfonation of a large number of substrates with very different structures ranging from flavonoid and phenolic acids to steroids and glucosinolates. In some cases, the sulfonation is required for biological activity (such as glucosinolates) while in others it seems to inactivate biological function (such as brassinosteroids and jasmonic acid) (Gidda et al., 2003, Marsolais et al., 2007, Rouleau et al., 1999).

Amino acid sequence alignment of plant and animal cytosolic SULTs revealed four conserved regions named region I to region IV (Varin et al., 1992). The results of site-directed mutagenesis studies showed that the catalytic domain is composed of conserved histidine, serine and arginine residues from region II and a lysine residue from region I, which together are responsible for the formation of an unstable ternary enzyme-PAPS-substrate complex and for the transfer of the sulfonate group to the substrate (Varin et al., 1992). The comparison of human and *Flaveria chloraefolia* flavonol SULTs and the results of the specificity of chimaeric enzymes allowed mapping of the substrate binding region to regions 2 and 3. The 3-D structure determined by X-ray crystal of many soluble SULTs and one membrane-associated

SULT have been solved (Negishi et al., 2001). The structures confirmed the importance of the amino acid residues that were identified by site-directed mutagenesis.

In an effort to elucidate the function of plant SULTs, our laboratory initiated a small scale functional genomics project using the plant *Arabidopsis thaliana*. Data mining of the sequenced genome of Arabidopsis indicated the presence of 17 putative ST coding genes. The phylogenetic tree of the Arabidopsis SULTs is shown in Figure 1. The deduced protein sequences of the 17 SULT-coding genes were divided into seven groups according to their similarities. Among the 17 genes, seven have been characterized as following: flavonoid SULT (At3g45070) (Gidda and Varin,2006), desulfoglucosinolate SULTs (At1g74100, At1g74090, At1g18590) (Piotrowski et al., 2004), hydroxyjasmonate SULTs (At5g07010) (Gidda et al., 2003) and brassinosteroid SULTs (At2g03760 and At2g14920). There is also one locus (At3g51210) that codes for a truncated protein.

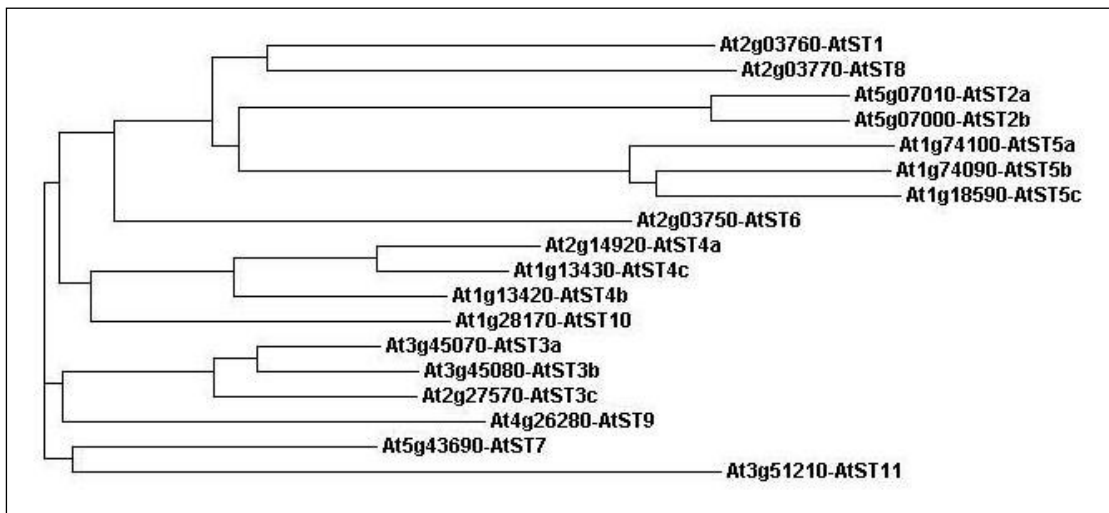


**Figure 1. Phylogenetic tree of *Arabidopsis thaliana* sulfotransferases.** The amino acid sequences of 17 SULTs and one truncated protein were grouped using the Clustal W program (<http://www.ebi.ac.uk/Tools/clustalw2>). Seven groups are created according to their sequence similarities.

## 1.2 *AtST4* subfamily

Based on the proposed guidelines for sulfotransferase nomenclature (Blanchard et al., 2004), the *AtST4* subfamily has three members: *AtST4a* (At2g14920), *AtST4b* (At1g13420) and *AtST4c* (At1g13430). Molecular studies of the *AtST4* subfamily have shown that the three genes are expressed mainly in roots (Marsolais et al., 2007). *AtST4a* (At2g14920) has 80% amino acid sequence identity with *AtST4c* (At1g13420) and 71% amino acid sequence identity with *AtST4b* (At1g13420).

Efforts to identify the substrates of *AtST4a*, *AtST4b*, and *AtST4c* indicate that *AtST4a* was catalytically active with brassinosteroids *in vitro*. Although sulfated brassinosteroids were not detected in plant extracts suggesting that *in vivo* the substrate

of AtST4a is not a brassinosteroid. Despite their high amino acid sequence identity, neither AtST4b nor AtST4c exhibited any activity with brassinosteroids (Marsolais et al., 2007). Analysis of microarray data showed that *AtST4b* specifically is expressed in roots of young seedlings and is up-regulated by cytokinins, these results were confirmed by transcript expression analysis that will be presented in the results section. A metabolite study of *AtST4b* knockout plants revealed that cadabicine is the substrate of AtST4b and that the formation of cadabicine sulfate is induced by the exogenous application of cytokinins (Kodashenas et al., 2010). *AtST4b* knockout plants exhibited a more robust growth than wild type plants with a better developed root system (Fig 2). They also exhibited a reduced sensitivity to the exogenous application of cytokinins (Kodashenas et al., 2010).

*AtST4c* knockout plants were found to flower approximately 5 days earlier than wild-type when grown under long day photoperiod (Kodashenas et al., 2010). This result was not observed in *AtST4a* and *AtST4b* knockout plants (Fig 2). This phenotype was highly reproducible and observed both in soil and *in vitro* grown plants.

In addition to the alteration of flowering time, *AtST4c* knockout plants exhibited abnormal root development with shorter primary roots and a reduction in the number of lateral roots. Several unsuccessful attempts were made to identify the substrate of AtSt4c. It was soon realized that AtST4a and AtST4c might generate the same product since the sulfonated metabolomes of *AtST4a* knock out and *AtST4c* knock out mutant lines were identical to wild type plants (Kodashenas et al., 2010). There is much

experimental evidence suggesting that this might be the case. First, their substrate co-elute during the HPLC purification of acid-hydrolyzed root extracts. Second, their radio-labeled products have the same retention time during reverse phase chromatography and finally, their product have the same relative mobility on TLC (Kodashenas et al., 2010). To test this hypothesis and further characterize the substrate of AtST4a and AtSt4c, AtST4ac double knockout line was generated by crossing homozygous *AtST4a* and *AtST4c* T-DNA insertion lines.

It is well known that cytokinins mediate opposite effects on shoot (positive) and root (negative) growth (Werner et al., 2009). The analysis of the Genevestigator Arabidopsis Microarray database showed that *AtST4c* is slightly repressed following the exogenous application of the cytokinin *t*-zeatin (genevestigator.org), suggesting that *AtST4c* might play a positive role in root growth and that this effect is inhibited by cytokinins.



**Figure 2. Flowering phenotype of *Arabidopsis thaliana* wild-type and knockout**

**lines** Wild-type (upper left) and *AtST4c* knockout (upper right), *AtST4a* knockout (lower left) and *AtST4b* knockout (lower right) plants 21 days after germination. Early flowering phenotype was observed in *AtST4c* knockout plants.

### **1.3 Regulation of flowering time in *Arabidopsis thaliana***

One objective of this research project was to characterize the relationship between *AtST4c* and the regulation of flowering time in *Arabidopsis*. A short review of the known mechanisms that regulate flowering time in *Arabidopsis* is presented to justify the choice of the *Arabidopsis* mutant lines used in this project.

In annual plants, the timing of the transition from vegetative growth to reproductive development is crucial for reproductive success and it is tightly controlled by environmental and endogenous signals (Torti et al., 2012). Because of its importance,

the elucidation of the molecular mechanisms that control this transition has attracted a lot of interest. Studies on the regulation of flowering time have a history of more than 100 years (Kobayashi and Weigel , 2007). The results of early pre-molecular studies indicated that the initiation of flowering is regulated by a “biological clock”, a concept that was first proposed by Bunning in the 1930s (Bunning et al., 1930). In this model, light was considered as an important external signal that could trigger the plant to flower. Apart from the length of the photoperiod, the quality of light and temperature were also proposed to play a significant role in the induction of flowering (Srikanth and Schmid , 2011).

The molecular mechanisms of flowering time regulation have been studied mostly in *Arabidopsis thaliana*. In the last 10 years, tremendous progress has been made in our understanding of the molecular regulation of flowering time. Based on the analysis of transgenic plants and on the isolation of loss-of-function mutant plants, approximately 180 genes have been implicated in flowering time control. Five major genetic pathways regulating the flowering transition were identified. The photoperiod and vernalization pathways control flowering in response to environmental stimuli such as day length and temperature. The gibberellin pathway induces flowering even in the absence of a favorable photoperiod. The autonomous pathway refers to endogenous regulators that are independent of the photoperiod and gibberellins pathways (Srikanth and Schmid, 2011). The age pathway which stimulates flowering in relation to the age of the plant has recently been added to the network. In order to control plant

flowering time properly, the signals from all of these pathways converge to regulate a small number of common targets, which have been referred to as floral integrator genes. The results of recent studies have shown that during floral induction, morphological changes of the meristem are associated with changes in the expression of the floral integrator genes (Fornara et al., 2010). So far, the mechanisms by which the different pathways communicate with the integrator genes are not well understood. Table 1 lists some of the integrator genes that are clearly playing a crucial role in floral induction. (Srikanth and Schmid, 2011)

Table 1. Some of the important floral integrator genes of *Arabidopsis thaliana*

	Gene Name	Function	References	Comments
<b>FT</b>	<i>FLOWERING LOCUS T</i> <u>AT1G65480</u>	Activator	(Kardailsky et al., 1999),(Kobayashi et al., 1999)	Activator of flowering; long distance signal from leaf to shoot apex
<b>LFY</b>	<i>LEAFY</i> <u>AT5G61850</u>	Activator	(Blazquez and Weigel, 2000),(Weigel et al., 1992)	Integrates signals from the GA, photoperiod and age pathways. Essential for floral organ formation
<b>SOC1</b>	<i>SUPPRESSOR OF OVEREXPRESSION OF CONSTANS 1</i> <u>AT2G45660</u>	Activator	(Samach et al., 2000),(Moon et al., 2003) ,(Lee et al., 2008) ,(Lee & Lee., 2010)	Integrates signals from photoperiod, vernalization and GA pathways. Following translocation to nucleus, SOC1 binds to the <i>LFY</i> promoter
<b>API</b>	<i>APETALAI</i> <u>AT1G69120</u>	Activator and repressor	(Abe et al., 2005, Kaufmann et al., 2010, Wigge et al., 2005)	Regulates genes required for organ formation in a tissue-specific manner while repressing the genes required for transition to flowering.

*CONSTANS* (*CO*) is the key gene of the photoperiod dependent promotion pathway (An et al., 2004), It encodes a putative zinc finger transcription factor (Putterill et al., 1995) and its expression is under the control of the circadian clock. Much evidences

shows that the *FLOWERING LOCUS T (FT)* (Table 1), one of the floral integrator genes, is a primary target of *CO* in leaves (Figure 3). For example, in the phloem of *CO* overexpressing plants, *FT* mRNA abundance is increased and the plants flower earlier. In contrast, *ft* mutations strongly suppress the early flowering of the *CO* overexpressor lines (An et al., 2004). Similarly, over-expression of *CO* in *ft* mutant plants does not rescue the late flowering phenotype, but when *FT* is overexpressed in *co* mutants, the late flowering phenotype of the latter is completely rescued (Yoo et al., 2005). Interestingly, further analysis of the *FT* gene showed that it is not acting in leaves but might promote flowering at the shoot meristem (Srikanth and Schmid, 2011). Several scenarios have been proposed to explain how *FT* might act far from its site of synthesis (Corbesier et al., 2007) (Jaeger and Wigge, 2007). *FT* interacts with the bZIP transcription factor FD in the meristem and *fd* mutations reduce the early flowering phenotype of plants overexpressing *FT* (Abe et al., 2005). *CO* is not the only gene to regulate *FT* expression and several repressors of *FT* such as *APETALA2 (AP2)* have been identified. *AP2* is best known for its role in the specification of flower organ identity as well as a negative regulator of *SOCI* in the control of the establishment of flower meristem identity. (Okamuro et al., 1997).

Besides *AP2*, *FT* is also a direct target of *FLOWERING LOCUS C (FLC)* which encodes a MADS box protein (Figure 3) (Searle et al., 2006)(Helliwell et al., 2006). *FLC* acts as a potent repressor of flowering, but the strength of its effect varies among

different *Arabidopsis* ecotypes. *FLC* expression is silenced by the vernalization pathway in response to lengthy exposure to low temperature (Fornara et al., 2010). Finally, genes such as *FCA* belonging to the autonomous pathway promote flowering by repressing *FLC* expression (Fornara et al., 2010).

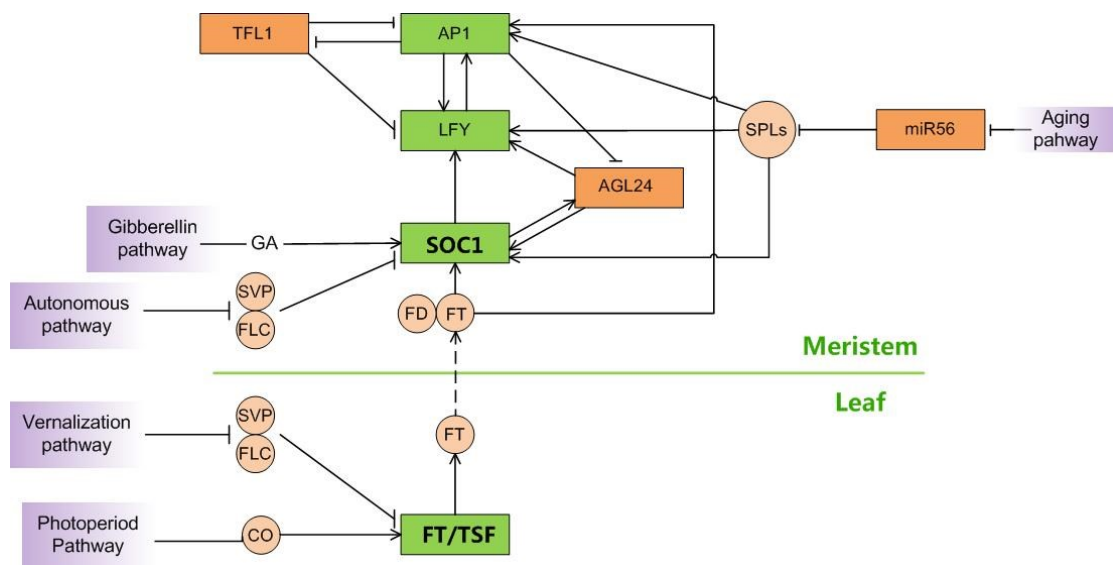


**Figure 3. Integration of the flowering time pathways.** The arrows indicate activation while the vertical bars indicate repression. The flowering pathways are indicated by the purple boxes. The floral integrators, such as *FT*, *SOC1*, *LFY*, *API* are also shown in green. This figure is modified from (Fornara et al., 2010)

Another target of *FLC* at the shoot meristem is *SUPPRESSOR OF OVEREXPRESSION OF CONSTANS 1 (SOC1)*, which is also one of the known floral integrator genes (Table 1). *SOC1* is a positive regulator of flowering at the shoot apex (Moon et al., 2003). *SOC1* activation occurs rapidly when plants are shifted from short to long photoperiods, and this activation requires *FT* (Fornara et al., 2010). *SOC1* is a

target not only for *FT*, but also for at least four different pathways as well (Figure 3). For example, it was reported that the expression of *SOCI* is up-regulated by the GAs and aging pathways, and down-regulated by the autonomous pathway( Moon et al., 2003). As shown in Figure 3, GA regulates *SOCI* expression at several levels by promoting expression of *SOCI* induced genes such as *AGAMOUS LIKE 24 (AGL24)* and at the same time down-regulating floral repressors such as *SHORT VEGETATIVE PHASE (SVP)* (Li et al., 2008). As plants grow, the aging pathway will be activated, resulting in increasing concentrations of the SQUAMOSA PROMOTER BINDING LIKE (SPL) protein, which promotes flowering by activating floral integrator genes such as *SOCI* (Figure 3)(Srikanth and Schmid, 2011). In the autonomous pathway, the MADS box proteins encoded by *FLOWERING LOCUS C (FLC)* and *SVP* form a heterodimer which represses *SOCI* transcription (Figure 3)(Fujiwara et al., 2008, Li et al., 2008).

The activation of *SOCI* in the meristem leads to changes in the expression of genes encoding other transcription factor genes, such as *LEAFY (LFY)* (Table 1). *LFY* was first recognized for its function in the flower meristem. *lfy* mutants show leaf-like structures replacing the floral organs, and transgenic plants overexpressing *LFY* flower earlier than wild-type plants (Weigel and Nilsson, 1995). *LFY* mRNA was detected in both the floral meristem and young leaf primordia suggesting that it plays a role in flower development and in the control of vegetative growth (Blazquez et al., 1997). *LFY* is not only a direct target of *SOCI* (Lee et al., 2008), but also of multiple other

pathways. For example, part of the flower-stimulating activity of gibberellins is due to an activation of *LFY* expression (Blazquez et al., 1998). *LFY* is also activated by *SQUAMOSA PROMOTER BINDING LIKE (SPL)*, a member of the aging pathway (Gou et al., 2011).

Flowering induction mediated by the floral integrators ends with the initiation of flower development and does not require the maintenance of flowering signals for a long period of time. *APETALAI (API)* is one of genes that can define the commitment to flowering, which means that by the time *API* is expressed, floral determination has occurred (Hempel et al., 1997).

In summary, floral transition is regulated by a precise genetic network consisting of different pathways responding to environmental stimuli and endogenous cues. To date, great advances have been made in our knowledge of the molecular mechanisms that control the floral transition and many genes in the network have been identified and characterized in detail (Figure 3).

#### **1.4 Purpose of the present study**

The three members of the *AtST4* subfamily are expressed exclusively in roots, and are regulated by cytokinins. However, only *AtST4c* knockout plants show an early flowering phenotype suggesting that the *AtST4c* SULF might play a role in the switch

from vegetative to reproductive growth. The purpose of the present study is to identify the endogenous substrate of AtST4c and to characterize the biological functions of *AtST4c* in the control of flowering time. Several approaches were used to identify the substrate of *AtST4c*. The comparison of extracts from wild type and *AtST4ac* double knock out mutant plants allowed characterization of the substrate of AtST4c using Liquid Chromatography-Mass Spectrometry (LC-MS). The structure of the AtST4c sulfonated product was predicted by high resolution MS/MS from the analyses of the fragmentation pattern of the parent molecule. Finally, qRT-PCR was used to study the regulation of several crucial flowering integrator genes such as *SOC1*, *APETALA 1*, *APETALA 2* and *LFY* in the *AtST4c* knockout plants. The expression of *AtST4c* was also studied in *Arabidopsis* plants harboring mutations in flowering integrator genes.

## Chapter 2- Materials and Methods

### 2.1 Materials

Seeds of wild type *A. thaliana*, ecotype Columbia 0 (Col-0) were obtained from Lehle seeds (USA). The Arabidopsis lines carrying T-DNA insertions in the coding sequence of *AtST4a* (GABI\_177E08) was obtained from Gabi-Kat (<http://www.gabi-kat.de/>), and *AtST4c* (FLAG\_334F06) from INRA (<http://www.inra.fr/>). The two knockout mutant lines were generated in a Col-0 background. The *AtST4a/AtST4c* double mutant was obtained by crossing the homozygous *AtST4a* and *AtST4c* knockout lines.

The *Lfy* mutant line (Stock number: CS6278) was obtained from the Arabidopsis Biological Resource Center (ABRC)

### 2.2 Methods

#### Plant growth conditions

Arabidopsis plants were grown either in soil or on vertical Petri dishes containing full-strength Murashige and Skoog (MS) medium (1% sucrose, 0.4% Gelrite, 0.05% MES, PH 5.7). For long day photoperiod experiments, the plants were kept for 16 hours under light a light intensity of  $\sim 130 \mu\text{mol m}^{-2}\text{s}^{-1}$  and 8 hours dark at. The temperature was kept at 20 °C during night-time and gradually increased to 22 °C during day-time. For short day conditions, the plants were kept for 8 hours under light at a light intensity of  $\sim 130 \mu\text{mol m}^{-2}\text{s}^{-1}$  and 16 hours dark

### **Seed sterilization**

The Arabidopsis seeds were sterilized by a 30 second immersion in 70% ethanol, followed by 5 minutes shaking in a mixture of 10% bleach and 0.02% SDS solution and several rinses with sterile distilled water. The seeds were then kept for 2-4 days at 4°C in dH<sub>2</sub>O before planting.

### **Validation of the *AtST4c* T-DNA insertion knockout lines**

The loss of the *AtST4c* transcript in the *AtST4c* knockout line was confirmed using reverse transcription polymerase chain reaction (RT-PCR) using a pair of primers designed to anneal to the *AtST4c* coding sequence. Total RNA was extracted from 20-day-old Arabidopsis root tissue using the RNeasy Plant Mini Kit (Qiagen). Before elution from the column, total RNA was treated with DNase I (Qiagen) for 15 minutes at room temperature to eliminate genomic DNA contamination. For the RT-PCR experiments, 2 µg of total RNA in RNase-free water was used. each reaction contains 1µl of 100 µM Oligo dT (20 mers) and 1µl of 100mM dNTP mix (Biolab) with incubation for 10 minutes at 65°C and subsequent cold on ice for 2 minutes. A mix of 4 µl 5X First Strand Buffer (Invitrogen), 1 µl dTT (100 mM), 1 µl RNase Out and 1 µl Superscript III Reverse Transcriptase 50 U/µl (Invitrogen) was added to each reaction, followed by 60 minutes incubation at 50°C. This procedure was followed by a 15 minute incubation at 70 °C to deactivate the enzyme. The synthesized cDNAs were then used in PCR reactions.

In the PCR reactions, the *ACTIN* genes were used as internal controls for RNA calibration. The amplification of the *ACTIN* cDNAs was conducted using 30 cycles of 1) denaturation at 94°C for 45 seconds, 2) primer annealing at 60°C for 45 seconds and 3) elongation at 72°C for 1 minute. A final extension at 72°C for 7 minutes followed the 30 cycles of amplification. The amount of cDNA, used as template for PCR, was adjusted after a preliminary calibration based on the level of the *ACTIN* PCR products. For *AtST4c*, we used 35 cycles of 1) denaturation at 94°C for 1 minute, 2) primer annealing at 56°C for 1 minute and 3) elongation at 72°C for 1 minute.

The following primers were used in the amplification reactions:

actin-Forward (5'-GCTGATGGTGAAGACATTCA-3')

actin-Reverse (5'-CATAGCAGGGGCATTGAAAG-3')

AtST4c-Forward (5'-CGCTTAAACTACCCTTGAAG-3')

AtST4c-Reverse (5'-AGAACAAAAACCACACATCA-3')

The primers were ordered from Integrated DNA Technologies (USA) and dissolved in DNase/RNase free water at a final concentration of 10 µM.

### **Phenotype analysis of *AtST4c*-knockout plants**

Wild-type (Col-0) and *AtST4c* knockout plants were grown under long day and short day conditions in growth chambers. The flowering time was calculated once the bolting shoot had reached 1cm in length. The number of siliques was measured 36 and 46 days after germination.

## **Expression, purification and *in vitro* assays of the AtST4c recombinant enzyme**

**Recombinant protein expression and purification:** The coding sequence of *AtST4c* was cloned previously in a bacterial expression plasmid pQE30 (Qiagen) and transformed into the *E. coli* strain XL1-blue. A culture of *E. coli* carrying this plasmid was grown to an  $O.D_{600} = 0.6$  and induced with 1mM Isopropyl  $\beta$ -D-1-thiogalactopyranoside (IPTG) for 10 hours at 22<sup>0</sup>C. Bacterial cells were collected by centrifugation and resuspended in lysis buffer (50 mM sodium phosphate, 0.3 M NaCl, 10 mM imidazole and 14 mM  $\beta$ -mercaptoethanol) (pH 8.0). The cells were lysed by sonication, and the recombinant proteins were recovered in the soluble fraction by centrifugation at 13,000 rpm for 20 minutes at 4<sup>0</sup>C. The soluble recombinant proteins were purified by affinity chromatography onto a nickel-nitrotriacetic acid agarose matrix (Qiagen) under native condition. Protein concentration was estimated using the Bradford Reagent (Bio Rad) with bovine serum albumin as a reference protein. To verify the solubility and evaluate the level of purity of the recombinant protein after chromatography, aliquots of the recombinant enzyme were subjected to 12% polyacrylamide gel electrophoresis according to the method of Laemmli (Laemmli, 1970)(Ossipow et al 1993). The proteins were visualized using Coomassie Blue staining.

***In vitro* enzyme assays:** Prior to enzyme assays, mild acid hydrolysis was performed on an aliquot of the extract to remove the sulfonate group from the extracted metabolites. 5 $\mu$ l of HCl was added to 50 $\mu$ l of metabolite extract and incubated at 95  $^{\circ}$ C

for 5 minutes. The reaction was stopped by adding of 5  $\mu$ l of 1M NaOH. In order to track the AtST4c reaction product during purification, we used radiolabeled PAPS as sulfonate donor.

Root metabolic extracts were used to purify the potential substrate of AtST4c and to later identify the reaction product. In a typical experiment, 500 mg of root tissue was extracted with an aqueous methanolic solution and the methanol evaporated under vacuum using a flash evaporator.

The reaction mixture (50  $\mu$ l) contained 50 pmol [ $^{35}$ S] PAPS (NEN Life science products, Boston, MA), 5 $\mu$ l of acid hydrolyzed plant metabolite extract (dissolved in 50% methanol) and approximately 2  $\mu$ g of recombinant enzymes (extracted in 50 mM Tris-Cl, pH 7.5).

The reactions were incubated at room temperature for 10 minutes and then stopped by the addition of 10  $\mu$ l of 2.5% acetic acid. The sulfonated reaction products were extracted with 2 ml ice-cold water saturated butanol and 100  $\mu$ l was counted for radioactivity using a liquid scintillation counter.

The butanolic layer was collected, lyophilized and re-suspended in 50% methanol for enzyme assays and for LC-MS experiments.

### **Transcript expression study of *AtST4c* in response to cytokinins**

For transcript expression analysis, 20-day-old plants were sprayed with 20  $\mu$ M *trans*-zeatin dissolved in 50% dimethylsulfoxide (DMSO) for 1 hour, 2 hours, 4 hours

and 6 hours. RNA samples were extracted from root tissue using an RNeasy Plant Mini Kit (Qiagen). SuperScript III reverse transcriptase from Invitrogen was used to generate cDNAs by the method described previously.

### **Quantitative RT-PCR**

Quantitative real-time RT-PCR was performed using the following gene-specific primers:

Actin-F: 5'-GATTCAGATGCCAAGAAGTCTTG-3'

Actin-R: 5'-TGG ATT CCA GCA GCT TCC AT-3';

FT-F: 5'-CTCAGGTTCAAAACAAGCCAAG-3'

FT-R: 5'-GCAGGGATATCAGTCACCAAC-3';

SOC1-F: 5'-GTGCTGACTCGATCCTTAGTATG-3'

SOC1-R: 5'- CAGTGCTTTGTGATGCTGAAG-3';

AP1-F: 5'-TTCCCAAGATAATGCCTCTG-3'

AP1-R: 5'-CTTGAACGCTATGAGAGGTAATC-3';

Leafy-F: 5'-GCGAAGATAGCGGAGTTAGGTTT-3';

Leafy-R: 5'-CTTCAAGCTCCTCGTCCTTCA-3';

AP2-F: 5'- TCCACAAGATCACAACCT CG-3'

AP2-R: 5'- TCCGGTTTGACCTAATCCAAG-3';

AtST4c-F: 5'-TCTCAACAGCTC AAAACCGG-3'

AtST4c-R: 5'-TGCACACGTACTACTACCT TG-3';

AtST4b-F: 5'- GATGCGCTTAAAGTACCGTTG-3';

AtST4b-R: 5'- AAGACTCGAACAAAGCCTCG-3'.

RT-PCR was performed using a MBI EVOLution 5\* EvaGreen qPCR Mix (MBI). For each sample, three replicates were used. The MBI hotstart DNA polymerase was activated by a 15 min incubation step at 95°C. All PCR reactions were performed using the Eco Real-Time PCR system from Illumina. A denaturation step of 15 min at 95 °C was followed by 40 cycles consisting of 10 seconds denaturation at 95°C, 15 seconds primer annealing at 60°C, and 15 seconds elongation at an initial temperature of 72°C gradually increasing to 95°C to create the melt curve.

The comparative ( $\Delta\Delta C_T$ ) method was used to compare gene relative expression levels.

The relative quantification value is expressed as  $2^{-\Delta\Delta C_T}$ , where  $\Delta C_T \text{ target gene} = C_T \text{ target gene} - C_T \text{ control (actin)}$ ,  $\Delta C_T \text{ reference gene} = C_T \text{ reference gene} - C_T \text{ control (actin)}$ ,  $\Delta\Delta C_T = \Delta C_T \text{ target gene} - \Delta C_T \text{ reference gene}$ .

### **Mass spectrometry**

Electrospray ionization tandem mass spectrometry (ESI-MS/MS) was used for analysis of the metabolite extracts from wild type and T-DNA insertion mutant lines. The recombinant enzyme-catalyzed reaction products were analyzed using neutral loss scan in the negative and positive mode in search of a parent ion which gave a neutral loss of 80 mass units (mass of the sulfonyl group). The analyses were performed on the Quattro

triple quadrupole from Micromass using a cone voltage of 20 eV and collision-induced dissociation (CID) energy of 35 eV (2.5 mTorr argon). Data acquisition and analysis were performed using the Masslynx software from Micromass.

To get structural information and accurate mass of the reaction products, we used the LTQ-Orbitrap from ThermoFisher. The analyses were performed using a cone voltage of 20 eV and a collision-induced dissociation (CID) energy from 28-35 eV, variable energy based on different parent compounds. Data acquisition was performed at the highest level of mass accuracy of the instrument. Data analysis was performed using the Xcalibur software from Thermo Fisher.

## Chapter 3- Results

### 3.1 Introduction

Preliminary results obtained in our laboratory indicated that *AtST4a* and *AtST4c* might have the same biochemical function. Their substrate and product co-eluted during HPLC purification and their sulfonated product co-chromatographed on TLC. However, our previous efforts to identify the structure of their product were unsuccessful.

To elucidate the biochemical and biological function of *AtST4c*, we used several T-DNA insertion lines. The *AtST4c* (FLAG\_334F06) knockout line was obtained from INRA (<http://www.inra.fr/>) while the *AtST4a* (GABI\_177E08) knockout line was obtained from the Gabi-Kat collection (<http://www.gabi-kat.de/>). The *AtST4ac* double mutant was generated in our laboratory according to the method described by Higuchi et al., 2004.

The results obtained will be discussed in three sections. The first section describes the phenotype of the *AtST4c* T-DNA insertion line. The second section describes the characterization of the endogenous substrate of AtST4c and finally, the third section describes the results of our studies of the regulation of *AtST4a*, *AtST4b* and *AtST4c* expression in different mutant backgrounds affected in flower development.

## **3.2 Characterization of *AtST4c* biological function**

### **3.2.2 Identification of homozygous *AtST4c* T-DNA insertion line**

The *AtST4ac* double knockout line was generated by crossing homozygous *AtST4a* and *AtST4c* T-DNA insertion lines. The *AtST4ac* mutant line carries T-DNA insertions 737 and 870 bases downstream of the translation start sites of *AtST4a* and *AtST4c*, respectively. In both cases, the insertion separates the regions encoding the sulfotransferase catalytic domain (region I) from the region encoding the PAPS binding domain (region IV) (Figure 4A). RT-PCR analysis of mRNAs isolated from the homozygous line confirmed the absence of *AtST4c* expression. The *AtST4c* transcript could be detected in extracts from wild-type plants (col-0) but not in extracts from the *AtST4ac* double knockout line (Figure 4B).

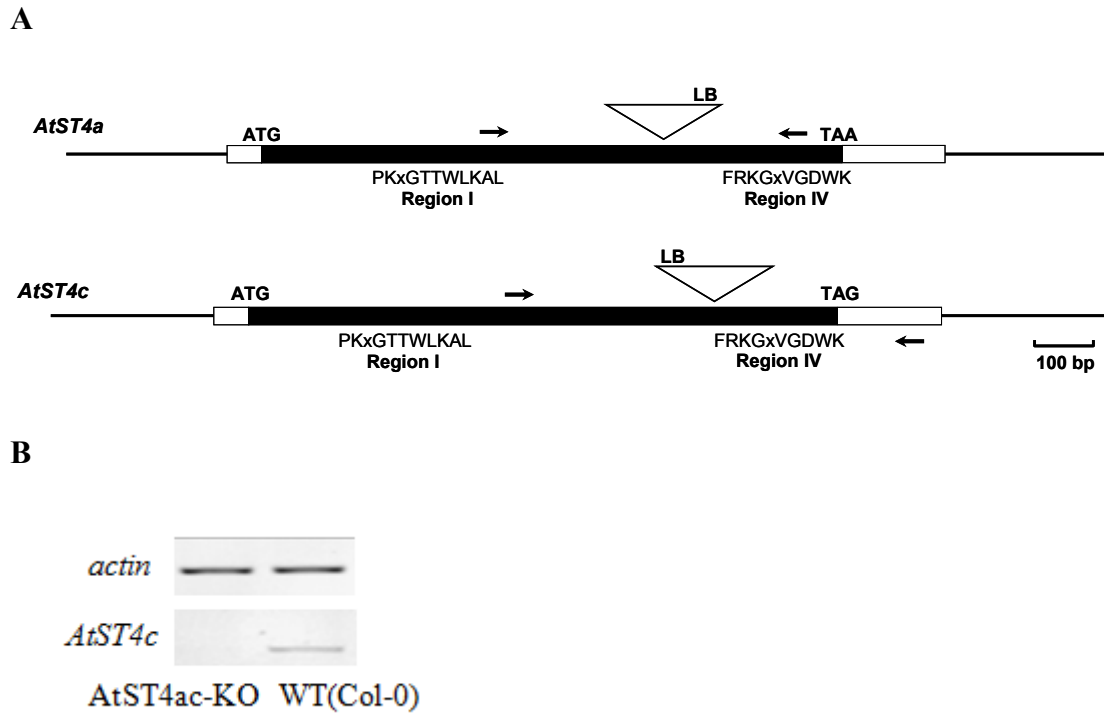


**Figure 4. Characterization of the *AtST4ac* double mutant line.**

- (A) A schematic model representing the position of the T-DNA insertions in *AtST4a* and *AtST4c*.** Black boxes: exons, white boxes: 5' and 3'UTRs, triangles: T-DNA insertion sites, arrows: gene-specific primers, LB: T-DNA left border. The consensus sequence for region I (PKxGTTWLKAL) and region IV (FRKGxVGDWK) were used to identify the regions involving in catalysis and PAPS binding.
- (B) RT-PCR analysis of *AtST4c* transcription.** RNA was extracted from roots of 20-day-old wild-type (col-0) or *AtST4ac* homozygous knockout mutant plants. The *ACTIN* gene is used as an internal positive control.

### 3.2.3 Phenotype of the Arabidopsis *AtST4ac* double mutant line

#### Flowering time

It has been shown previously that under long day conditions, *AtST4c* knockout plants flowered earlier than wild type (Kodashenas et al., 2010). Wild type plants will start to flower 25 to 26 days after germination and will have 12 to 14 leaves at the onset of flowering. In contrast, the *AtST4ac* double knockout plants initiated flowering 21 days after germination and have 6 to 7 leaves at the onset of flowering (Fig 5,6). Flowering under long photoperiods is under the control of the photoperiod promotion pathway in which the transcriptional activator *CONSTANS* plays a key role (An et al., 2004). In order to characterize further the link between *AtST4c* and flowering initiation, we evaluated the flowering time of the *AtST4ac* double knockout plants grown under short photoperiods. The results of several experiments have shown that flowering under short photoperiods is independent of the photoperiod promotion pathway and does not require a functional *CONSTANS* gene (An et al., 2004).

Under short day conditions, wild-type plants flowered approximately 92 days after germination, while *AtST4ac* double knockout plants flower after approximately 70 days (Fig 5).

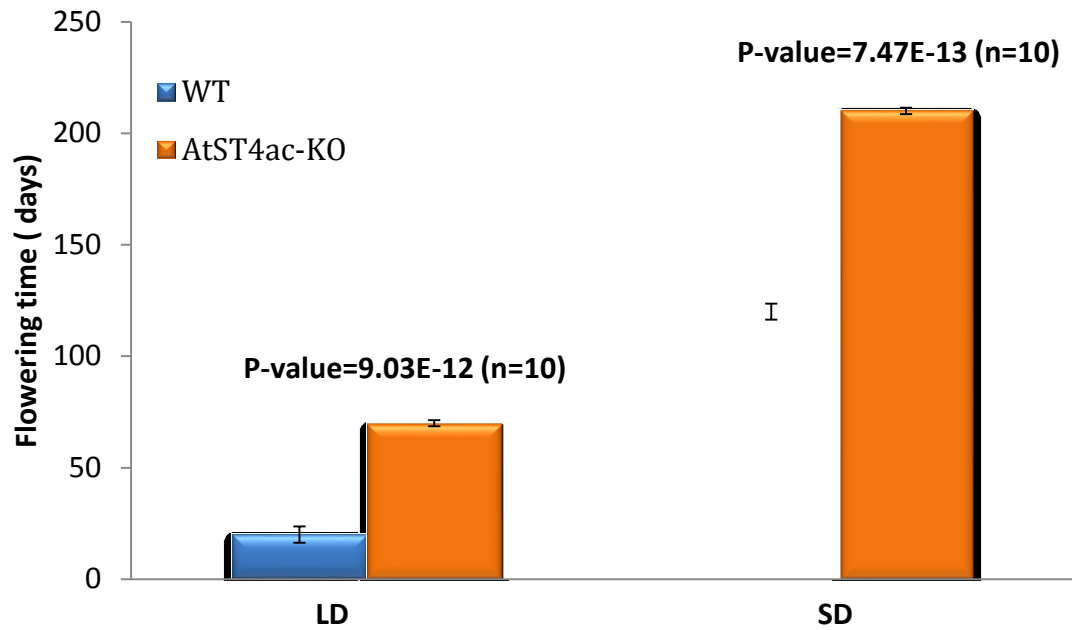


**Figure 5. Flowering time behavior of wild type and *AtST4ac* double knockout**

**plants.** LD: long day conditions, 16 hr light and 8 hr dark; SD: short day conditions, 8 hr light and 16 hr dark. Analysis of significance between wild type and mutant lines was performed using the Student's t-test.



**Figure 6. Early flowering phenotype of *AtST4ac* double knockout plants (right) compared to wild-type (left) plants grown under long day conditions.**

## Seed production

The number of siliques on the inflorescences of wild-type and *AtST4ac* double knockout plants was evaluated 36 and 46 days after germination. As expected for an early flowering mutant, the number of siliques (~360% and 76% more siliques at 36 and 46 days, respectively) was higher in *AtST4ac* double knockout plants. (Fig.7). No apparent change was observed in the shape and length of the siliques between the two genotypes. However, analysis of mature siliques showed that there was a ~17% reduction in seed number in the siliques of *AtST4ac* double knockout plants as compared to siliques from wild-type plants.

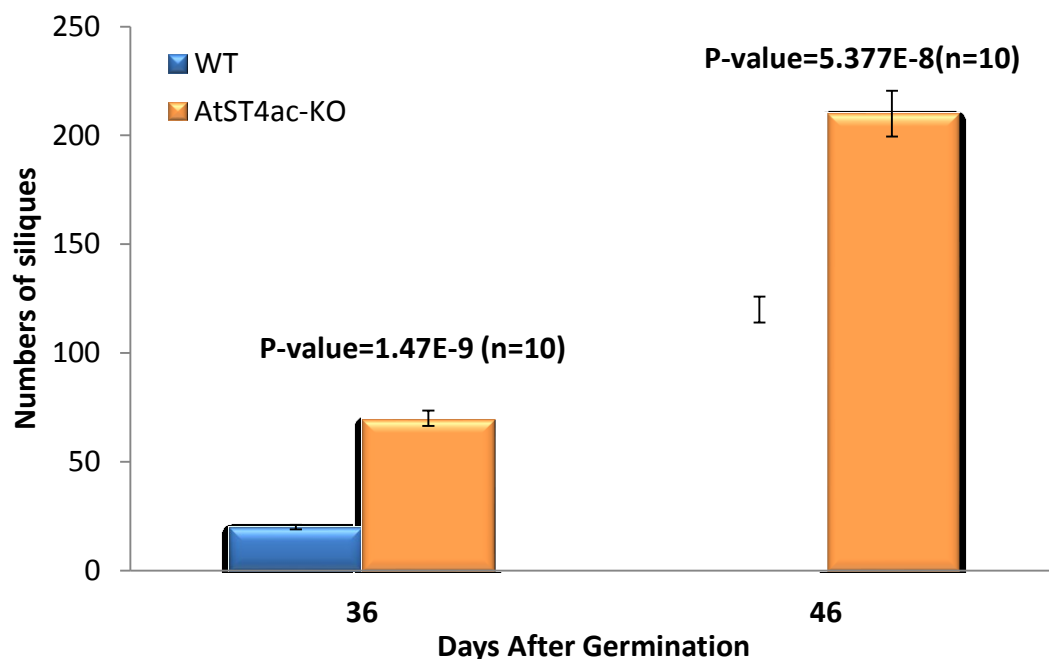


**Figure 7. Reproductive development of *AtST4ac* double knockout plants.**

Number of siliques per plant 36 and 46 days after germination. Analysis of significance between wild-type and mutant lines was performed using the Student's t-test.

### **3.3 Biochemical characterization of AtST4c**

#### **3.3.1 Introduction**

Several experimental strategies were used to characterize the substrate and product of AtST4c. First, we used the recombinant AtST4c enzyme expressed in *E. coli* to partially purify the endogenous substrate from total root metabolite extracts from wild-type plants. Then we defined the chromatographic behavior of the product of the reaction using HPLC. These initial experiments were followed by a thorough comparative analysis of the sulfonated metabolite profiles of wild-type, *AtST4a*, *AtST4c* and *AtST4ac* knockout mutant plants using LC-MS and LC-MS/MS.

#### **3.3.2 Expression and assay of the AtST4c recombinant enzyme**

To determine the biochemical function of the enzyme encoded by *AtST4c*, the coding sequence was cloned into the bacterial expression vector pQE30 (Qiagen). This plasmid generates a 6 His-tag fusion at the N-terminus of the recombinant protein. The his-tag was used for affinity purification of the enzyme on a Ni-agarose column. As expected, the partially purified recombinant enzyme migrated at a molecular weight of approximately 38 kDa on SDS-PAGE (Fig. 8).

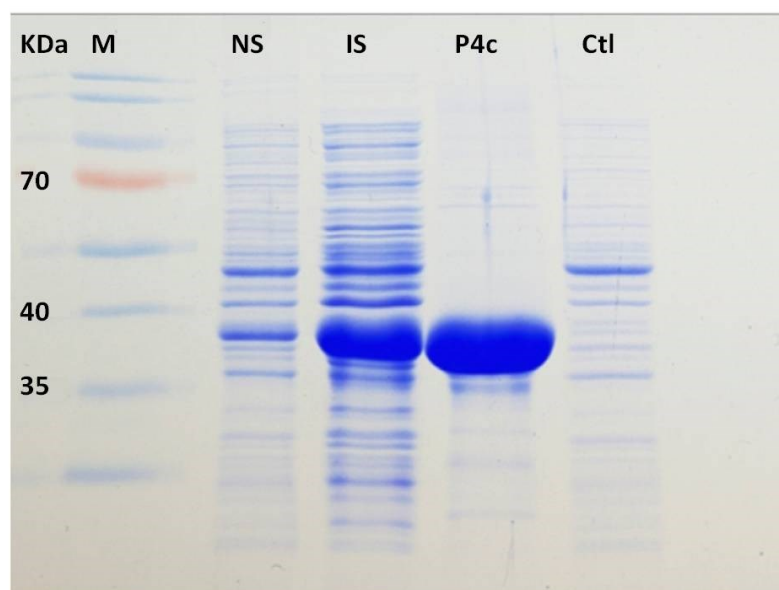


**Figure 8. SDS-PAGE of purified AtST4c recombinant enzyme.**

M: protein markers, NS: non-induced soluble proteins, IS: induced soluble proteins ,  
P4c: NI-agarose purified AtST4c , ctl: pQE 30 empty vector.

### **3.3.3 HPLC purification of the substrate and enzymatic reaction product of AtST4c**

To identify the elution time of the AtST4c substrate, the acid-hydrolyzed root extract was fractionated by High Performance Liquid Chromatography (HPLC). Individual fractions were collected and assayed with the recombinant AtST4c enzyme. The results show that highest enzymatic activity was detected with fraction 25 representing approximately 80% of the total (Fig. 9).

The product of the enzymatic reaction with fraction 25 was further chromatographed on HPLC to find the elution time of the product. As previously mentioned, the availability of the radiolabeled product facilitates the tracking during purification by

reverse phase HPLC. Figure 10 shows that two peaks eluting at 24 and 33 minutes can be detected in the gradient (Fig 10).

### **3.3.4 Neutral loss mass spectrometry of the AtST4c purified product**

Neutral loss mass spectrometry is a method that identifies, out of a complex mixture, parent molecules that lose a fragment of defined mass when the collision energy is increased. It is well known that sulfonated compounds can easily be detected using this experimental approach because of their tendency to lose an 80 dalton fragment corresponding to the sulfonyl group ( $\text{SO}_3^-$ ). Figure 11 shows the spectrum of a neutral loss experiment conducted with crude root extracts from wild-type and AtST4ac double knockout plants. A major ion (more than 98% of total ion count) having a mass-to-charge ratio ( $m/z$ ) of 516 daltons in positive mode  $[\text{M}+\text{H}]$  is present in both extracts. This compound has previously been characterized in our laboratory as the product of the AtST4b enzymatic reaction. Another ion having a  $m/z$  of 498 daltons  $[\text{M}+\text{H}]$  is present in the wild-type spectrum but absent from the AtST4ac double knockout extract (Fig.11, lower graph) suggesting that AtST4a, AtST4c or both enzymes are responsible for its synthesis. Figure 12 shows that the ion with the  $m/z$  of 498 daltons elutes at 16 minutes during LC-MS. Interestingly, neutral loss experiments conducted with metabolite extracts of *AtST4a* and *AtST4c* single knockout plants generated spectra that were identical to the wild type ones supporting

the idea that *AtST4a* and *AtST4c* are sulfonating the same substrate *in vivo* (data not shown).

### 3.3.5 LC-MS/MS analysis of the AtST4c purified product

To elucidate the chemical structure of the compound having an  $m/z$  of 498 daltons  $[M+H]$ , a wild-type root extract was subjected to reverse phase liquid chromatography-tandem mass spectrometry (LC-MS/MS) analysis. Initially, the fragmentation pattern was obtained using a nano LC coupled to an Orbitrap mass spectrometer at the Centre for Biological Applications of Mass Spectrometry (CBAMS, Concordia University). Figure 13 shows the fragmentation pattern of the putative AtST4c enzymatic product. In the negative electrospray mode, the compound produced a deprotonated molecular ion at  $m/z$  496 daltons ( $[M-H]$ ). The MS/MS fragmentation of this compound gave major fragment ions at  $m/z$  416, 374 and 345 daltons. The molecular ion at  $m/z$  416 daltons is due to the cleavage of the sulfonate moiety from the parent ion ( $m/z$  496). Further fragmentation of the 374  $[M-H]$  ion produced ions at  $m/z$  of 294, 222, 164 and 150 daltons. Further fragmentation of the major ion having a  $m/z$  of 345 daltons resulted in ions with  $m/z$  of 222 and 121 daltons. Figure 13 shows the structure of the individual fragments elucidated by Dr. Jurgen Schmidt from the Institute of Plant Biochemistry (Halle, Germany) using Fourier Transform Ion Mobility Spectrometry (FT-IMS). The predicted structure contains a 6 carbon sugar linked to benzoic acid and guanine. It is important to note

that the MS analyses are not providing sufficient information to establish the exact position of the linkage between the sugar and the other parts of the molecule. This compound has never been reported to occur in nature.

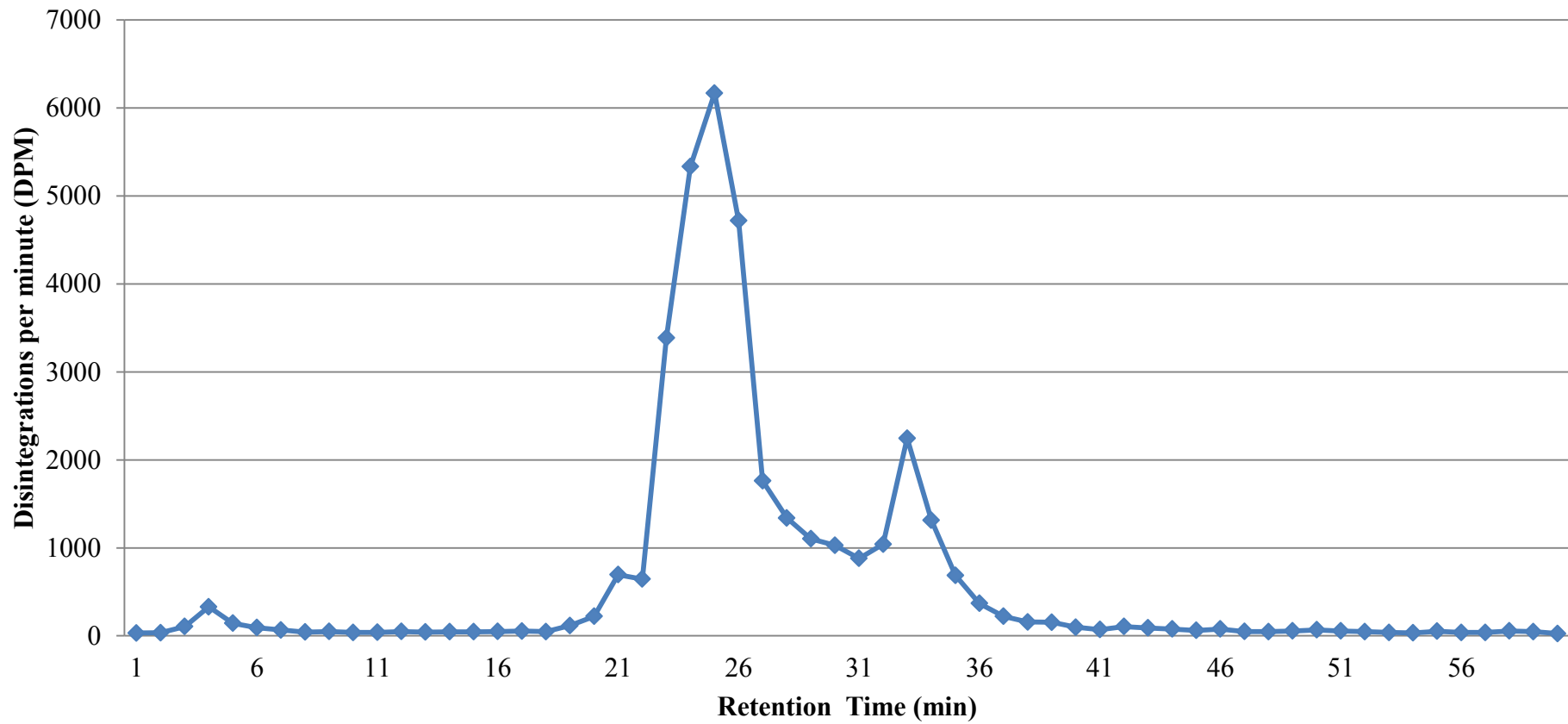


**Figure 9. Enzymatic activity profile of the HPLC fractionated acid hydrolyzed root extract. Fractions 25 and 33 showed the highest enzyme activity.**

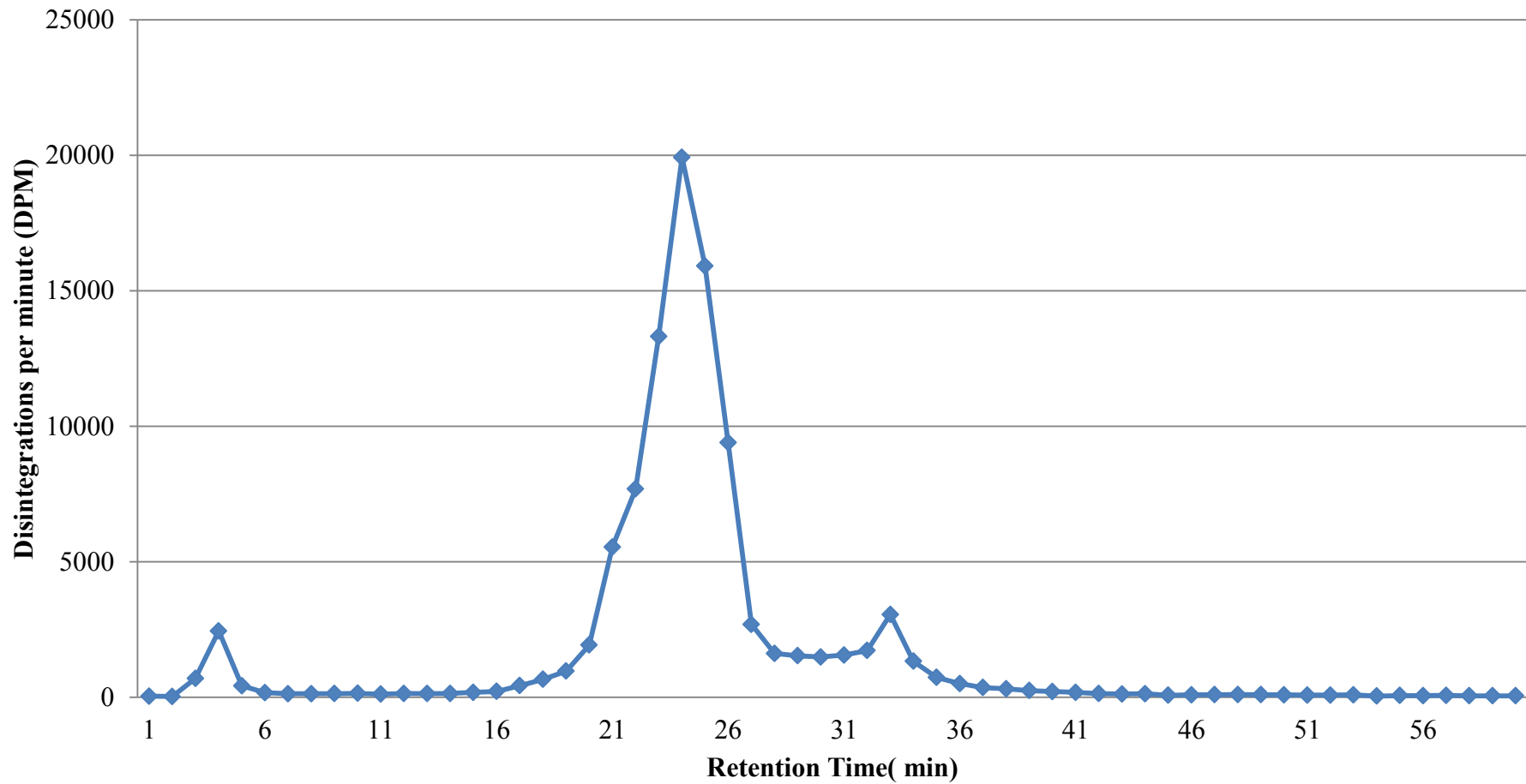


**Figure 10.HPLC purification of the AtST4c radiolabeled enzymatic product.** The highest radioactivity was recovered in fraction 24.

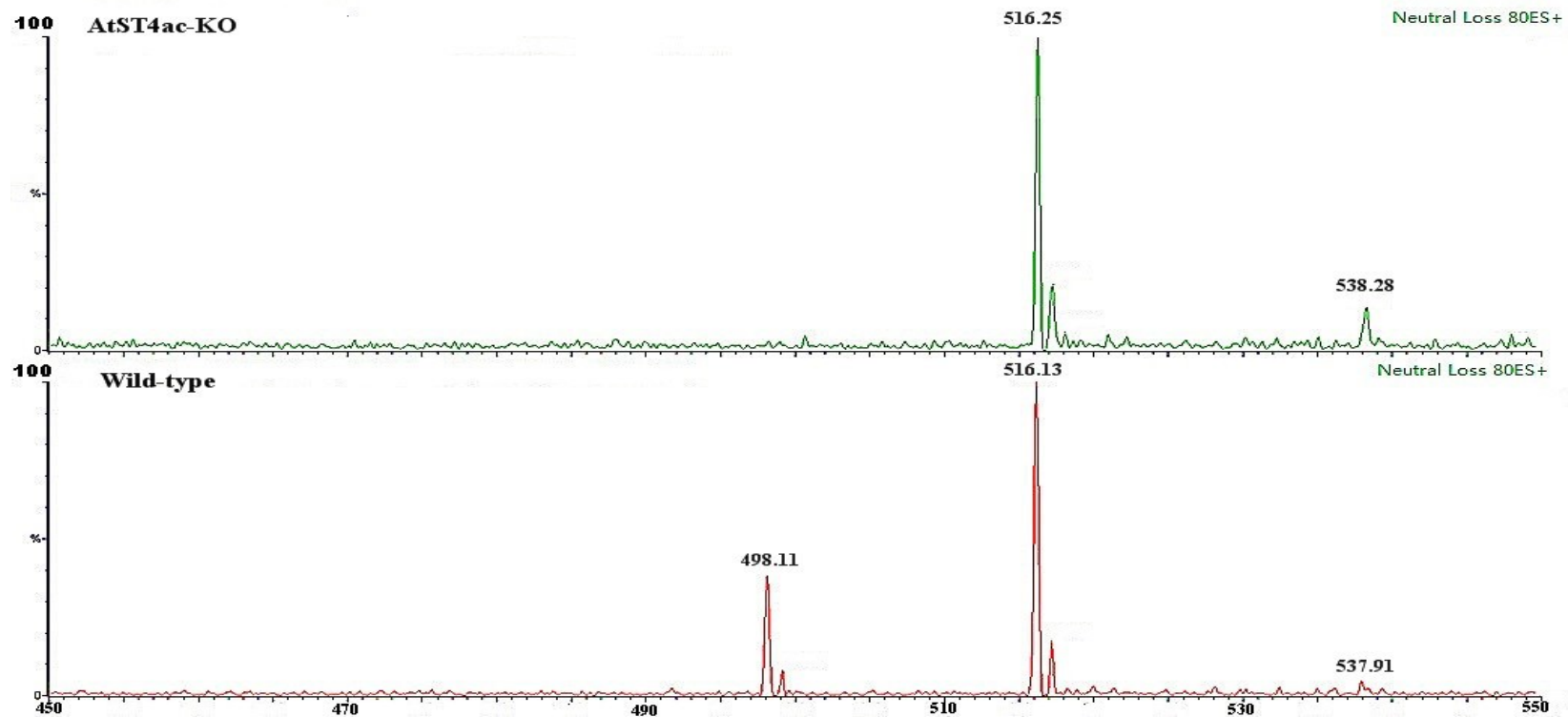


**Figure 11. Mass spectrometry of wild-type and *AtST4ac* double knockout crude root extracts.** Neutral loss spectra of root extracts from wild-type (lower graph) and *AtST4ac* double knockout (upper graph) plants in positive mode. The major peak at m/z 516 daltons corresponds to cadabicine sulfate. The arrow points to a molecular ion having a m/z of 498 daltons [M+H] that is missing in the *AtST4ac* double knockout spectrum.

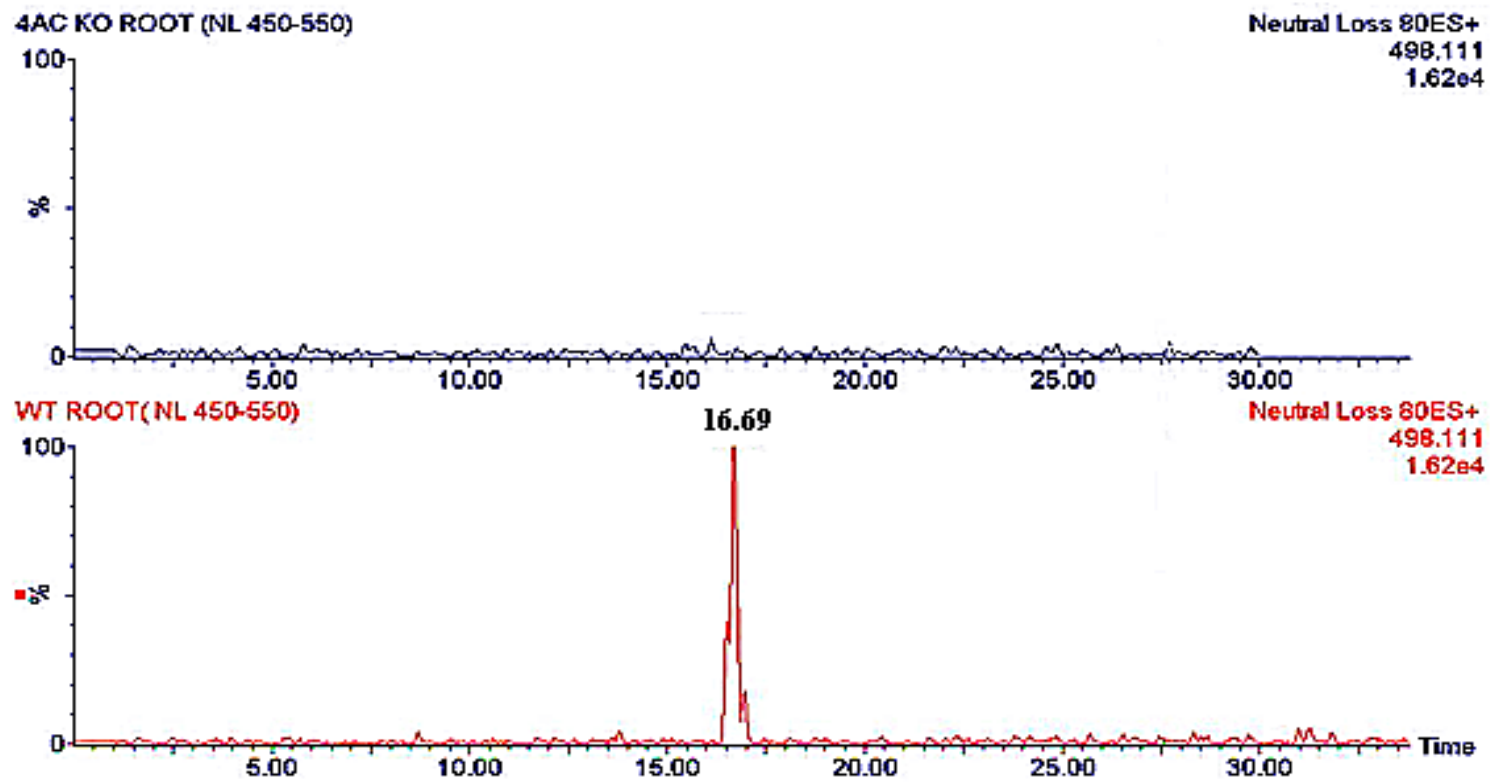
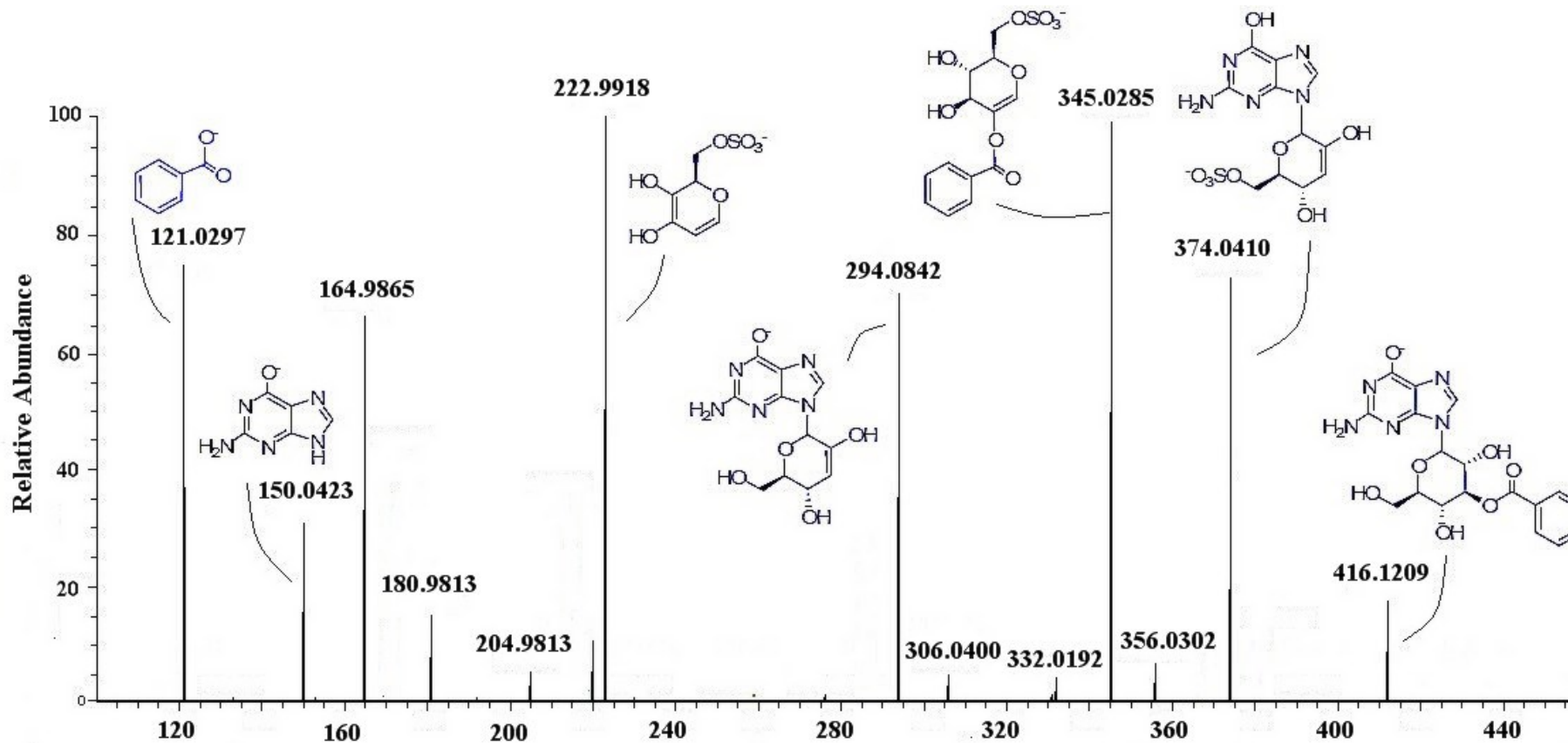


Figure 12. Chromatogram of the ion with an  $m/z$  of 498 daltons  $[M+H]$  from wild-type (bottom) and *AtST4ac* double knockout (top) root extracts.



**Figure 13. LC-MS/MS spectrum of the AtST4c sulfated product in negative mode.** MS/MS of the product with a m/z of 496 daltons [M-H].

The structures of some of the fragments are shown.

### **3.4 Regulation of *AtST4c* expression**

#### **3.4.1 *AtST4a* and *AtST4c* expression in different tissues of wild-type Arabidopsis at different development stages.**

The available microarray data from Genevestigator initially showed that the expression of *AtST4a* and *AtST4c* was predominantly taking place in the root system. To confirm this expression pattern and study the expression level at different growth stages, quantitative RT-PCR was performed (Fig.14). Our results show that *AtST4a* and *AtST4c* are mainly expressed in roots with the highest level of expression at the flowering stage. Very little expression is observed in the aerial tissue. However, *AtST4c* expression in the aerial tissues is higher before flowering time. *AtST4a* has a lower level of transcription than *AtST4c* in all tissues and at all development stages (Fig.14).

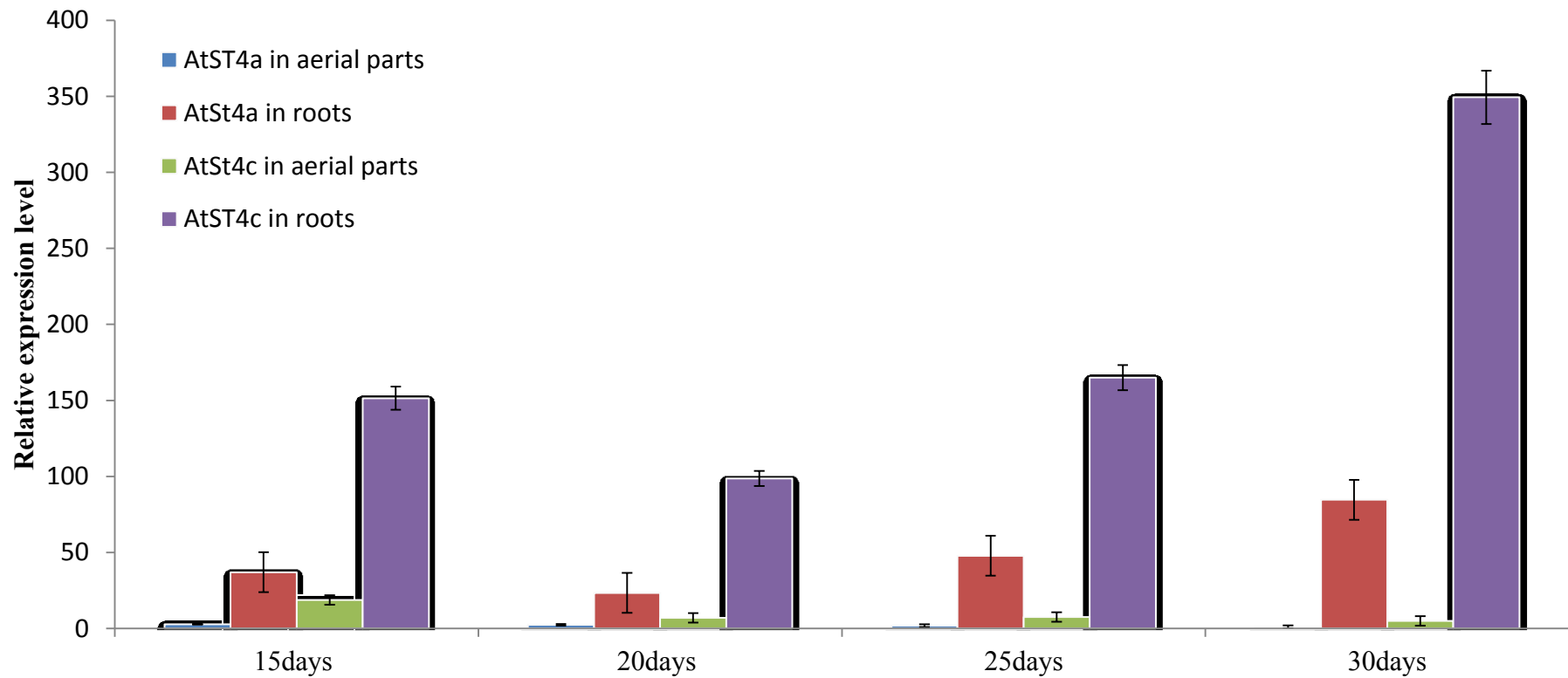


**Figure 14. Expression profiles of AtST4a and AtST4c in aerial parts and roots of Arabidopsis at different developmental stages.** Total RNA was extracted from different tissues of the plant. Quantitative RT-PCR was performed with gene-specific primers. *ACTIN* was used as internal constitutive control. The data represent the mean values of three independent biological replicates.

### 3.4.2 Transcript expression study of *AtST4c* response to cytokinins

Cytokinins regulate many important aspects of plant development (Werner and Schmulling, 2009). In Arabidopsis, cytokinins mediate the responses to many extrinsic factors, such as light conditions and availability of nutrients and water in the root system (Werner and Schmulling, 2009). Genome-wide microarray data showed that members of the *AtST4* subfamily are regulated by cytokinins (Hoth et al., 2003, Kiba et al., 2005). For example, it has been shown that *AtST4b* is strongly induced by cytokinins in seedlings of Arabidopsis. In contrast, *AtST4a* and *AtST4c* are slightly repressed by cytokinins. Quantitative RT-PCR was performed to further define the effect of cytokinins on the expression of the *AtST4* family members. Total RNA was extracted from roots of 16-day-old plants that were treated with 10 $\mu$ M *t*-zeatin for various periods of time. The upper panel of Figure 15 shows that 1 hour after the treatment with *t*-zeatin, *AtST4b* transcript levels start to increase with a maximum 17 fold induction after two hours. In contrast, *AtST4a* and *AtST4c* expression levels decreased in response to the treatment (Figure 15, lower panel).

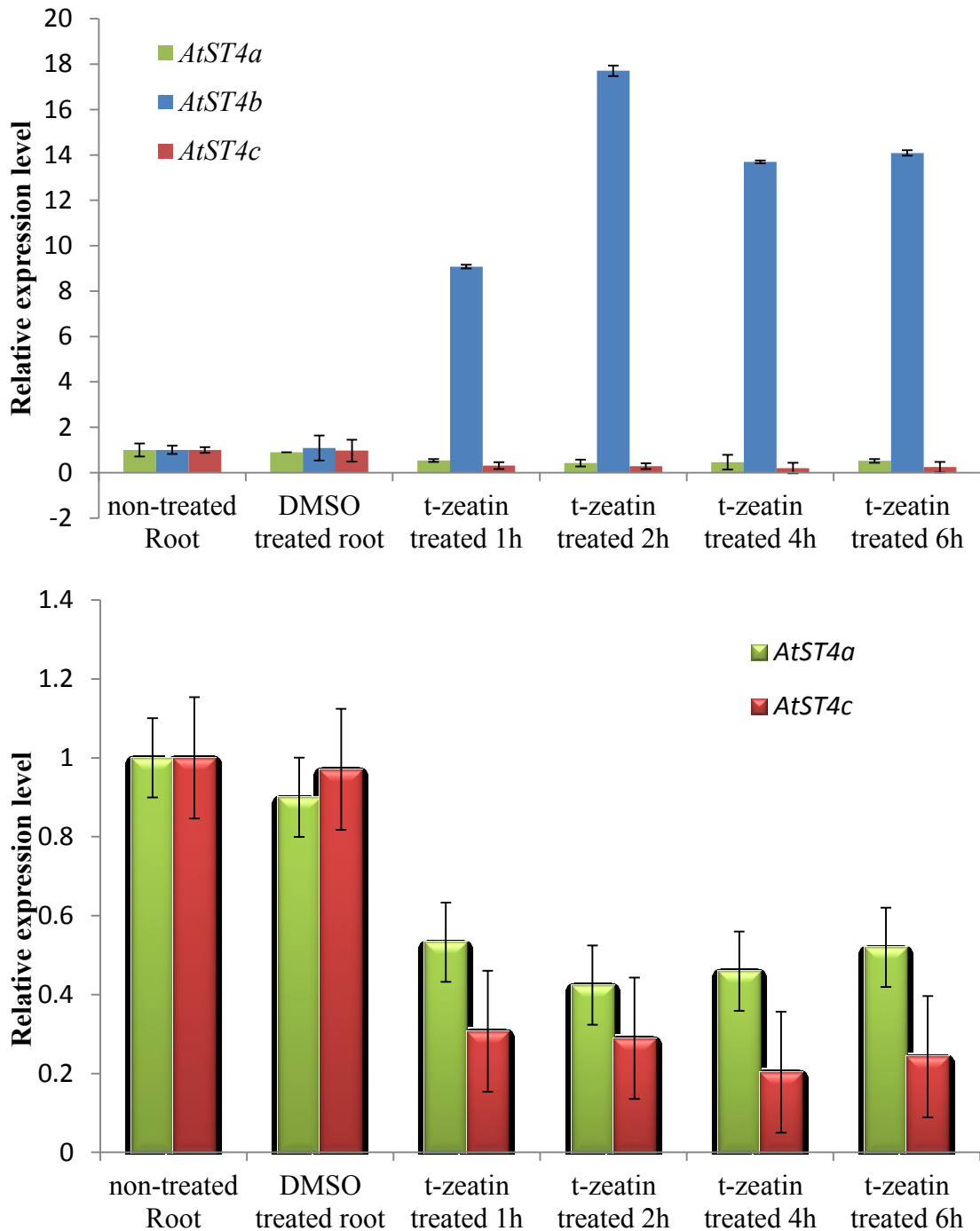


**Figure 15. Quantitative RT-PCR profiles of AtST4 subfamily members in response to cytokinins.** Total RNA was extracted from roots of 16-day-old Arabidopsis (Col-0) vertically grown on MS media non-treated or treated with 20 $\mu$ M t-zeatin for 1, 2, 4 and 6 hours. *ACTIN* was used as an internal constitutive control. The data represent the mean value of three independent biological replicates.

### **3.4.3 *AtST4c* expression in wild-type and *lfy* mutant plants.**

The switch from vegetative to reproductive growth is a crucial developmental transition that significantly affects the reproductive success of flowering plants (Mockler et al., 2004). In *Arabidopsis*, this transition is in large part controlled by the meristem identity regulator *LEAFY* (*LFY*). It has been reported that *LFY* is extensively expressed during the vegetative phase. Under long day conditions, there is an up-regulation of *LFY* at the onset of flowering. Under short-day conditions, *Arabidopsis* plants flower several weeks later than under long day conditions and *LFY* expression increases gradually until flowering starts (Blazquez et al., 1997). The exact mechanism by which *LFY* precisely controls the plant transition to flowering is not well understood yet. Since the *AtST4c* knockout mutant plants exhibit an early flowering phenotype, we tried to find out if there is a relationship between *LFY* and *AtST4c* expression. One possible hypothesis would be that *LFY* is a negative regulator of *AtST4c* expression. To test this hypothesis, we first used quantitative RT-PCR to measure the relative expression level of *AtST4c* and *LFY* in the aerial parts of wild-type plants.

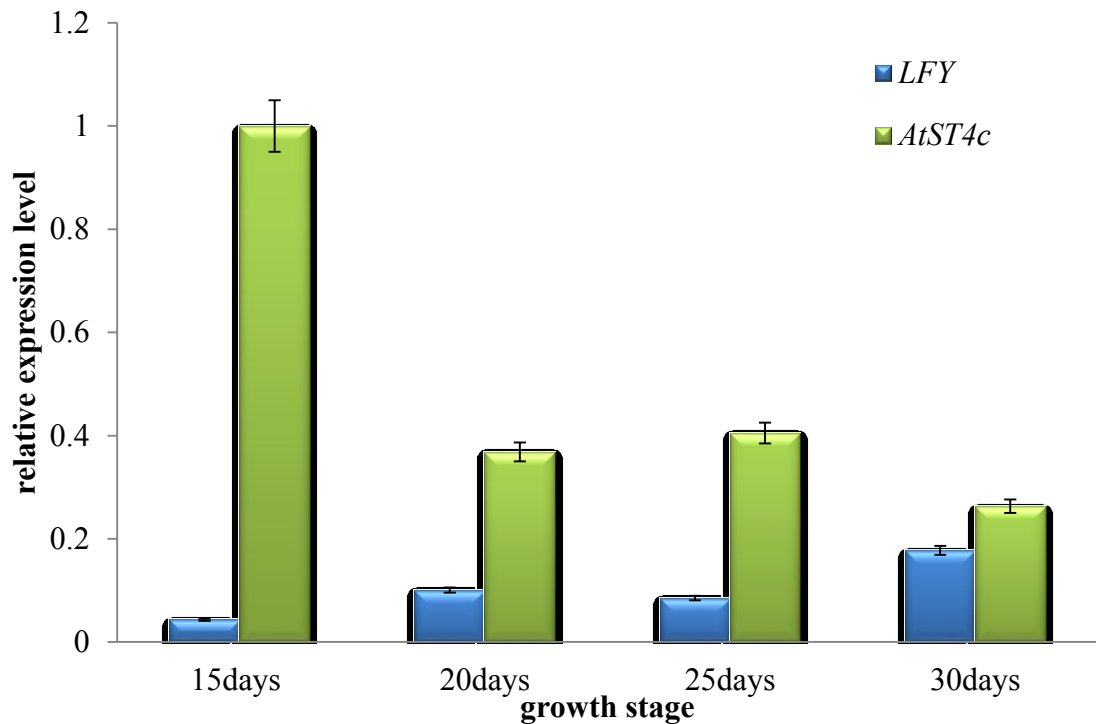


**Figure 16. Relative expression of *LEAFY* and *AtST4c* in wild-type Arabidopsis plants.** Plants were grown on MS medium under long day condition. *ACTIN* was used as internal constitutive control. The data represent the mean values of three independent biological replicates.

As shown in Fig.16, the expression of *AtST4c* decreases as the plant ages while the expression of *LEAFY* increases. These patterns of expression are consistent with the microarray data that can be retrieved from the Genevestigator web site. Even though the opposite expression behavior of the two genes fits with our proposed hypothesis, we cannot conclude that *LFY* regulates *AtST4c* expression.

To further test our hypothesis, we studied the expression of *AtST4c* in a plant line harboring a *lfy* loss-of-function mutation. If our hypothesis is correct, we should see an increased accumulation of the *AtST4c* transcript at all stages of growth in the *lfy* mutant plants. We used quantitative RT-PCR to compare the relative level of expression of

*AtST4c* in the aerial parts and the root system of wild type and *lfy* mutant plants at different developmental stages. As shown previously, *AtST4c* expression decreases in wild-type aerial parts as the plants age (Fig. 17). In contrast, *AtST4c* expression increases in the root system as the plant ages. *AtST4c* expression is lower in the root system at all tested developmental stages of the *lfy* mutant as compared to wild-type plants. The same behavior is observed for the aerial parts up to day 25. However, there is a strong increase of *AtST4c* expression in the aerial parts of the *lfy* mutant plants at day 30. Based on these results, we cannot conclude that *LFY* is a negative regulator of *AtST4c* expression at least until day 25 which represents the stage when wild-type *Arabidopsis* plants would normally initiate flowering. The strong increase of *AtST4c* at day 30 in the *lfy* mutant is associated with the growth of the bolting structures that generate multiple scale-like leaves instead of the normal inflorescence (Fig 16).

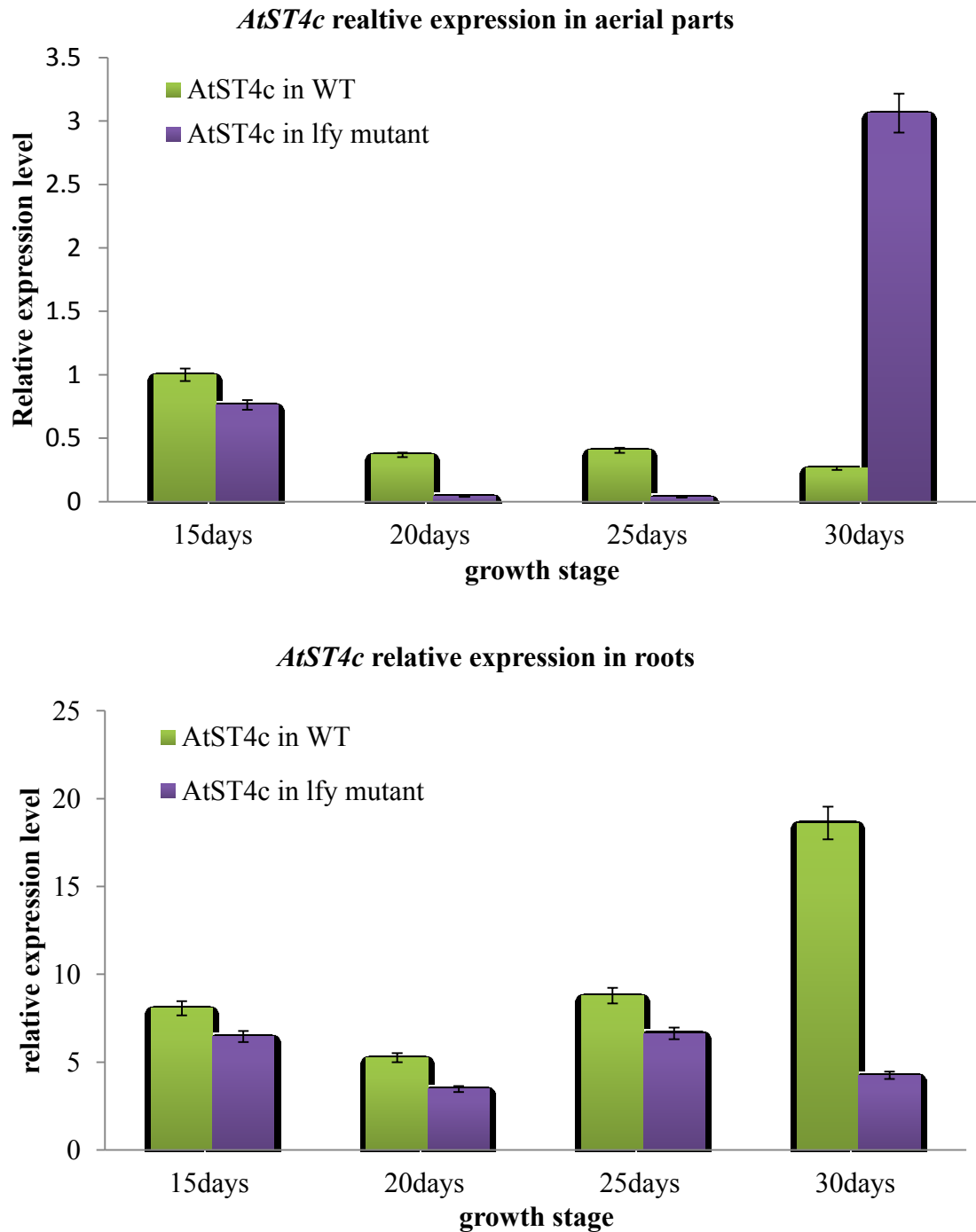


**Figure 17. Relative expression levels of *AtST4c* in wild-type and *lfy* mutant of *Arabidopsis* as determined by quantitative RT-PCR. Plants were grown on MS medium under long day conditions. *ACTIN* was used as an internal constitutive control. The data represent the mean values of three independent biological replicates.**

#### **3.4.4 Expression profile of genes regulating flowering time in the AtST4c knockout mutant.**

As we have seen in the introduction, the transition from vegetative growth to reproductive development in *Arabidopsis* is regulated by the photoperiod, the autonomous, vernalization, gibberellins and age pathways (Mockler et al., 2004). These pathways interact simultaneously to regulate the expression of a set of genes critical for floral initiation. Previous genetic and molecular studies demonstrated that *APETALA1*(*API*), *APETALA2*(*AP2*), *LEAFY*(*LFY*) and *SUPPRESSOR OF OVEREXPRESSION OF CONSTANS 1* (*SOC 1*) play a key role in the establishment and maintenance of flower meristem identity as integrators of the flowering pathways (Okamuro et al., 1997). To further characterize the role of *AtST4c* in the control of flowering time, we studied the expression of these key genes in the *AtST4c* knockout plants.

##### ***LEAFY***

In wild-type plants, the expression of *LEAFY* increases as the plant ages with a maximum expression observed at day 30. These results are in agreement with the results that can be retrieved from the Genevestigator database. A similar trend is observed in the *AtST4c* knockout plants. However, the level of expression of *LEAFY* is significantly higher at days 20, 25 and 30 in the mutant compared with the wild-type plants (Fig.18a). These results are in agreement with what would be predicted for mutant plants which are flowering earlier than wild-type.

##### ***APETALA 1***

In wild-type plants, the expression of *APETALA 1* increases with development with a maximum observed at day 30 (Fig.18a). A similar behavior is observed in the *AtST4c* mutant plants. However, the level of expression of *APETALA 1* is significantly higher

in the knockout plants at all time points that were studied (Fig. 18a). Again, these results are in agreement with what would be predicted for mutant plants which are flowering earlier than wild-type plants.

### ***SOC 1***

*SOC 1* expression increases gradually as the plants age in both wild-type and *AtST4c* knockout plants. Only minor differences in *SOC 1* expression are observed between that wild-type and the mutant plants (Fig. 18b). This result is surprising considering the key role of *SOC 1* in the integration of the flowering signal from all the pathways that promote flowering. We were expecting a higher level of expression of *SOC 1* earlier in development in the early flowering *AtST4c* mutant plants.

### ***APETALA2***

*APETALA2* expression increases sharply at day 25 in wild-type plants. The increase corresponds to the time of initiation of flowering in wild-type Arabidopsis. A similar increase is observed in the *AtST4c* knockout plant. However, a significant decrease in *APETALA2* expression is observed at day 20 in the mutant plants. This growth stage coincides with the initiation of flowering in the *AtST4c* knockout plants (Fig.18b). It is important to note that the level of expression of *APETALA2* is relatively low in Arabidopsis at all growth stages and that only minor differences are observed in the *AtST4c* knockout mutant (Fig. 18b).

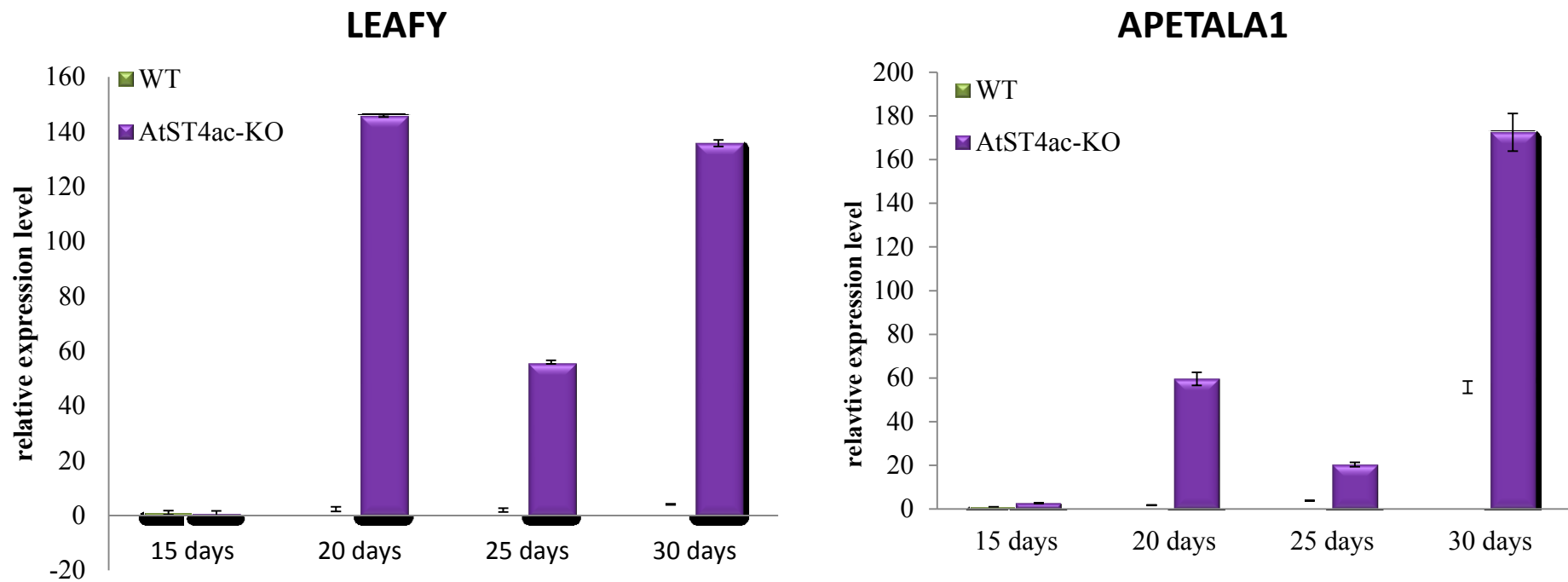


**Figure 18 (a).** Relative expression patterns of the flowering genes *LEAFY* and *APETALA1* in *AtST4c* knockout plants grown under long day condition. *ACTIN* was used as an internal constitutive control. The data represent the mean values of three independent biological replicates.

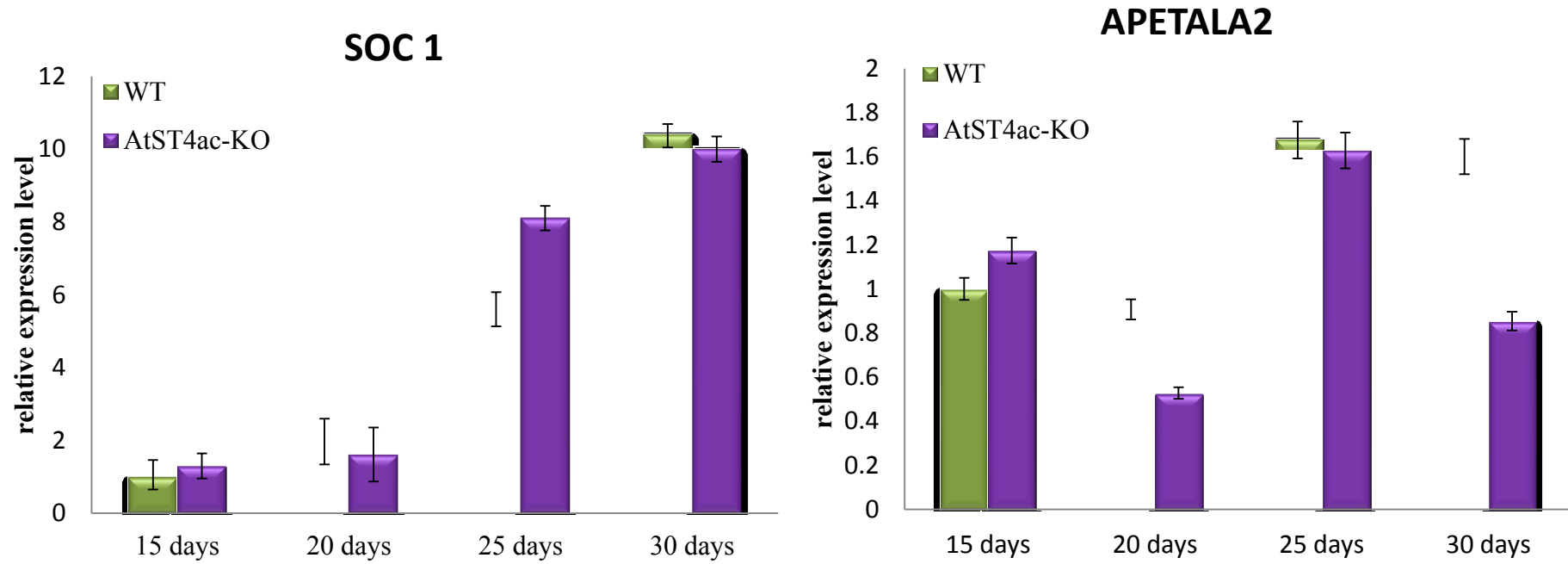


**Figure 18 (b).** Relative expression patterns of the flowering genes *APETALA2* and *SOC1* in *AtST4c* knockout plants grown under long day condition. *ACTIN* was used as an internal constitutive control. The data represent the mean values of three independent biological replicates.

## Chapter 4- Discussion

In *Arabidopsis*, the members of the *AtST4* subfamily of sulfotransferases are expressed in the root system and are regulated by cytokinins. To try to elucidate their function, we used a combination of biochemical and molecular approaches. First, the three coding sequences were cloned in bacterial expression vectors and recombinant proteins were produced in *E. coli*. This work allowed the study their biochemical function *in vitro* to try to elucidate the structure of their substrates. We also took advantage of the T-DNA insertion library to isolate plants missing one or the other of the three genes and to analyze their phenotype. Previous analyses of a T-DNA insertion mutant of *AtST4c* revealed a distinct phenotype as compared to the other members of the *AtST4* subfamily (Kodashenas et al., 2010). *AtST4c* knockout mutant plants were found to flower 5-6 days earlier than wild type plants when grown under long photoperiod (Fig. 2). This represents a reduction of approximately 20% in vegetative growth time and suggests that *AtST4c* plays a role in the repression of flowering. In addition, *AtST4c* knockout plants produce a smaller root system and have fewer leaves at the time of flowering indicating a more general role in the control of vegetative growth in all tissues of the plant. In contrast, a T-DNA insertion in *AtST4a*, the closest relative of *AtST4c* did not give rise to a visible phenotype (Kodashenas et al., 2010).

### **Biochemical function of AtST4c**

One of the most important objectives of this research project was to identify the substrate and product of the enzyme encoded by *AtST4c*. Several experimental strategies were used to reach this objective. One of the most powerful approaches was to compare metabolite profiles between mutant and wild-type plants using LC-MS. This work is facilitated by the distinct signature of sulfonated molecules in mass spectrometry using the neutral loss method. The loss of the sulfonate ion during fragmentation generates a daughter molecule that is 80 daltons lighter than the parent molecule. This method was used successfully for the identification of the substrate and product of AtST4b, another member of the *AtST4* subfamily. A molecular ion corresponding to cadabicine sulfate was completely absent from root extracts of *AtST4b* mutant plants allowing the unambiguous identify of the substrate and product of this enzyme. The same approach was initially used to characterize the substrate and product of AtST4a and AtST4c. The *AtST4ac* double mutant line was found to exhibit the same early flowering phenotype previously observed in the AtST4c knockout line. Metabolite profiling of a root extract from the *AtST4ac* double mutant line revealed the absence of a molecular ion having a mass of 498 daltons in positive mode [M+H] (Figure 11 and 12). The structure of this molecule was analyzed by high resolution mass spectrometry and was found to correspond to a 1-guanine 3-benzoic acid glucoside 6-sulfate (Figure 13). This molecule has never been reported to occur in nature. Unfortunately, the results of the mass spectrometry experiments do not allow the position of the linkage between the guanine, the benzoic acid, the sulfonate and the glucose molecule to be defined. However, the linkage positions proposed are based on the existence of other molecules containing part of the structure and having the linkages. For example, benzoic acid glucoside with a linkage at carbon 3 was found to

accumulate in the plant *Pteris ensiformis* (Chen et al., 2008). Although a guanine glucoside has never been reported to occur in nature, adenine linked to carbon 1 of glucose in the cytokinins benzyladenine-7-N-glucoside and isopentenyladenine-7-N-glucoside has been found in *Arabidopsis* (Hou et al., 2004). Finally, several molecules containing a glucose 6-sulfate have been reported to occur in algae, plants and mammals (Ale et al., 2011).

How can we reconcile that the two enzymes are probably sharing the same substrate *in vivo* with the differences observed in the phenotype of the *AtST4a* and *AtST4c* knockout lines? First, the metabolite profiling experiments were conducted with extracts of entire plants including roots and aerial parts. It will be important in future experiments to quantify the level of the *AtST4c* substrate and product in dissected tissues to see if there is an uneven distribution of the metabolites between the two knockout lines. Second, it also will be important to study the tissue localization of expression of the two genes in *Arabidopsis*. We cannot exclude the possibility that the control of flowering time is mediated by the substrate or product of *AtST4c* expressed in a very specific tissue or cell type during the maturation of the plant. It is also interesting to note that the level of expression of *AtST4c* is higher than that of *AtST4a* in *Arabidopsis*. This is especially true for the expression pattern of the two genes in the aerial parts of the plant (Fig. 14). It is possible that the higher level of expression of *AtST4c* in the aerial parts of the plant is crucial for the control of flowering time and is masked in the metabolite profiling experiments by the high level of accumulation of the sulfonated product in the root system.

### **Function of *AtST4c* in the control of flowering time**

In addition to the early flowering phenotype, an *AtST4c* loss of function mutation resulted in plants with shorter primary roots, a reduced number of lateral roots and

slightly smaller rosettes suggesting that *AtST4c* regulates vegetative growth positively and flowering time negatively. We also have shown that *AtST4c* is down regulated by the exogenous application of cytokinins (Fig.15). Interestingly, cytokinin-deficient plants show a late-flowering phenotype indicating that cytokinins play a positive role in plant flowering (Hoth et al., 2003). Based on our results, we can expect a higher level of expression of *AtST4c* in cytokinin-deficient plants which would coincide with the late flowering phenotype that is observed in these plants.

In order to understand how *AtST4c* participates in the control of flowering time, we have to learn how it affects genes that are known to regulate the switch from vegetative to reproductive growth. First, we analyzed the flowering time of *AtST4c* knockout plants grown under short photoperiods. Interestingly, the same early flowering phenotype was observed under long day and short day growth conditions (Fig.5). These results indicate that the effect of *AtST4c* on flowering time is not under the control of the photoperiod promotion pathway. Then we looked at the expression of key genes involved in flowering time in the *AtST4c* knockout line (Fig.18). As we have seen in the introduction, there are four pathways other than the photoperiod promotion pathway that regulate flowering time. The signals generated by all of these pathways converge at *SOC1* (Fig.3). Once activated, SOC 1 positively regulates *LEAFY* which then activates *APETALA1* expression. *LEAFY* plays a key role in the determination of the flowering meristem (Blazquez et al., 1997; Schultz and Haughn, 1991). *lfy* mutants show leaf-like structures replacing the floral organs, and transgenic plants overexpressing *LFY* flower early than wild type (Weigel and Nilsson, 1995). The results shown in Figure 18 indicate that the absence of *AtST4c* has a strong positive impact on *LEAFY* expression at days 20, 25 and 30 after germination. It is interesting to note that the strong induction of *LEAFY* coincides with the initiation of flowering in

the *AtST4c* knockout plants. The same pattern of induction is observed for the expression of *APETALA 1* (Fig.18a). This result is expected since *APETALA 1* expression is under the control of *LEAFY* (Kaufmann et al., 2010). *APETALA 1* has two functions in reproductive development. First, it is a meristem identity gene required for the switch from a vegetative to reproductive meristems. Once established, *APETALA1* expression is sufficient to maintain reproductive growth in absence of further stimulating signals. Second, it acts as an organ identity gene whose function is required for petal formation (Hempel et al., 1997) The up-regulation of *LEAFY* and *APETALA 1* in the *AtST4c* knockout background indicates that *AtST4c* acts upstream of the meristem identity genes in the control of flowering time. The fact that *LEAFY* and *APETALA 1* expression are not increased at day 15 suggests that there is another mechanism that prevents their expression early after germination. *TFL1* and *TFL2* are two candidate genes that can fulfill this function (Larsson et al., 1998).

We also looked at the expression of *SOC 1* in the *AtST4c* mutant background. *SOC 1* plays a key role as an integrator of the different signals coming from the five pathways regulating *LEAFY* expression. Surprisingly, the expression of *SOC 1* is not affected significantly by the loss of *AtST4c* function suggesting that the early flowering phenotype is not mediated by an increase in *SOC1* expression (Fig.18b). Finally, we also studied the expression of *APETALA 2* in the *AtST4c* mutant background. *APETALA 2* has a dual role as repressor of *SOC1* expression before flowering and as floral identity gene in petal development (Yoo et al., 2005). The results of our studies show little difference in *APETALA 2* expression between the *AtST4c* mutant and wild-type plants (Fig. 18b). Taken together, our results indicate that *AtST4c* participates in the negative regulation of *LEAFY* and *APETALA 1* and that this repression does not depend on the photoperiod promotion, the autonomous or the

gibberellins pathways. Further work will be required to position *AtST4c* in the network of genes regulating flowering time. One possible target would be the aging pathway that can regulate *LEAFY* independently from *SOC1* (Fig. 3). Alternatively, *AtST4c* might interfere with the repression of *LEAFY* mediated by *TFL 1*.

Two models can be proposed for the mode of action of *AtST4c*. In the first one, the sulfated product of the enzyme-catalyzed reaction is acting as a repressor of flowering. In the second one, the substrate is acting as an activator of flowering and its sulfonation inhibits its activity. In order to find out which hypothesis is valid, we will need to synthesize both molecules to test their biological activity *in vivo* and their effect on flowering time.

## **Perspective for future work**

### **Biochemical function of AtST4c**

Further work will be required to elucidate the structure of the substrate of AtST4c. The technology that we used does not allow the assignment of the position of the benzoic acid, the guanine and the sulfonate group on the sugar backbone. We will have to use NMR and/or organic synthesis to define without ambiguity the final structure. This will be a challenging project considering the low abundance of the metabolite in vivo and the requirement for extensive purification before conducting NMR experiments.

Much evidence indicates that *AtST4a* and *AtST4c* share the same substrate in-vivo. However, only the *AtST4c* knockout mutant flowers earlier than wild-type suggesting a different localization of the two enzymes. To address this question, it will be necessary to construct transgenic lines expressing a reporter gene under the control of the two different promoters. We should also quantify the sulfonated product in different tissues of the *AtST4a* and *AtST4c* knockout lines to see if it accumulates in different parts of the plant during development.

### **Biological function of AtST4c, its substrate and its product**

Our results suggest that *AtST4c* or its associated metabolites (substrate and product) are playing a role in the control of flowering time and we have observed different regulation patterns for *LEAFY* and *APETALA 1* in the *AtST4c* knockout plants. To refine our analyses, we have to be able to map the position of *AtST4c* in the network of genes controlling flowering. For example, it would be interesting to see if a mutation in the aging pathway influences *AtST4c* expression since this pathway can regulate directly the expression of *LEAFY* and *APETALA 1*. We could also conduct genome-wide transcription profiling experiments to have a complete picture of the genes having different expression patterns in the *AtST4c* knockout plants. Finally, the organic

synthesis of the substrate and product of AtST4c would allow feeding experiments to see if genes in the flowering network are affected by their incorporation in plant tissues.

## References

- Abe M, Kobayashi Y, Yamamoto S, Daimon Y, Yamaguchi A, et al. 2005. FD, a bZIP protein mediating signals from the floral pathway integrator FT at the shoot apex. *Science* 309: 1052-6
- Ale MT, Mikkelsen JD, Meyer AS. 2010. Important determinants for fucoidan bioactivity: a critical review of structure-function relations and extraction methods for fucose-containing sulfated polysaccharides from brown seaweeds. *Mar Drugs*. 2011;9(10):2106-30.
- An H, Roussot C, Suarez-Lopez P, Corbesier L, Vincent C, et al. 2004. CONSTANS acts in the phloem to regulate a systemic signal that induces photoperiodic flowering of Arabidopsis. *Development* 131: 3615-26
- Baek D, Pathange P, Chung JS, Jiang J, Gao L, et al. 2010. A stress-inducible sulphotransferase sulphonates salicylic acid and confers pathogen resistance in Arabidopsis. *Plant Cell Environ* 33: 1383-92
- Blanchard RL, Freimuth RR, Buck J, Weinshilboum RM, Coughtrie MW. 2004. A proposed nomenclature system for the cytosolic sulfotransferase (SULT) superfamily. *Pharmacogenetics* 14: 199-211
- Blazquez MA, Green R, Nilsson O, Sussman MR, Weigel D. 1998. Gibberellins promote flowering of Arabidopsis by activating the LEAFY promoter. *Plant Cell* 10: 791-800
- Blazquez MA, Soowal LN, Lee I, Weigel D. 1997. LEAFY expression and flower initiation in Arabidopsis. *Development* 124: 3835-44
- Blazquez MA, Weigel D. 2000. Integration of floral inductive signals in Arabidopsis. *Nature* 404: 889-92

- Bunning, E., K. Stern and R. Stoppel - Versuche über den Einfluss von Luftionen auf die Schlafbewegungen von Phaseolus - Planta 11-1930-67
- Corbesier L, Vincent C, Jang S, Fornara F, Fan Q, et al. 2007. FT protein movement contributes to long-distance signaling in floral induction of Arabidopsis. *Science* 316: 1030-3
- Fornara F, de Montaigu A, Coupland G. 2010. SnapShot: Control of flowering in Arabidopsis. *Cell* 141: 550, 50 e1-2
- Fujiwara S, Oda A, Yoshida R, Niinuma K, Miyata K, et al. 2008. Circadian clock proteins LHY and CCA1 regulate SVP protein accumulation to control flowering in Arabidopsis. *Plant Cell* 20: 2960-71
- Gidda SK, Miersch O, Levitin A, Schmidt J, Wasternack C, Varin L. 2003. Biochemical and molecular characterization of a hydroxyjasmonate sulfotransferase from Arabidopsis thaliana. *J Biol Chem* 278: 17895-900
- Gidda SK, Varin L. 2006. Biochemical and molecular characterization of flavonoid 7-sulfotransferase from Arabidopsis thaliana. *Plant physiology and biochemistry* : 44: 628-36
- Gou JY, Felippes FF, Liu CJ, Weigel D, Wang JW. 2011. Negative regulation of anthocyanin biosynthesis in Arabidopsis by a miR156-targeted SPL transcription factor. *Plant Cell* 23: 1512-22
- Helliwell CA, Wood CC, Robertson M, James Peacock W, Dennis ES. 2006. The Arabidopsis FLC protein interacts directly in vivo with SOC1 and FT chromatin and is part of a high-molecular-weight protein complex. *Plant J* 46: 183-92
- Hempel FD, Weigel D, Mandel MA, Ditta G, Zambryski PC, et al. 1997. Floral determination and expression of floral regulatory genes in Arabidopsis. *Development* 124: 3845-53

- Higuchi M, Pischke MS, Mahonen AP, Miyawaki K, Hashimoto Y, et al. 2004. In planta functions of the Arabidopsis cytokinin receptor family. *Proc Natl Acad Sci USA* 101: 8821-6
- Hoth S, Ikeda Y, Morgante M, Wang X, Zuo J, et al. 2003. Monitoring genome-wide changes in gene expression in response to endogenous cytokinin reveals targets in Arabidopsis thaliana. *FEBS Lett* 554: 373-80
- Hou B, Lim E, S.Higgins, J. Bowles, 2004. N-Glycosylation of Cytokinins By Glycosyltransferases of Arabidopsis thaliana. *The Journal of Biological Chemistry*, 279, 47822-47832.
- Laemmli U.K. 1970. Cleavage of Structural Proteins during the Assembly of the Head of Bacteriophage T4. *Nature* **227**, 680 - 685
- Larsson AS, Landberg K, Meeks-Wagner DR. 1998. The TERMINAL FLOWER2 (TFL2) Gene Controls the Reproductive Transition and Meristem Identity in Arabidopsis thaliana. *Genetics* June 1, 1998 vol. 149 no. 2 597-605
- Jaeger KE, Wigge PA. 2007. FT protein acts as a long-range signal in Arabidopsis. *Curr Biol* 17: 1050-4
- Kardailsky I, Shukla VK, Ahn JH, Dagenais N, Christensen SK, et al. 1999. Activation tagging of the floral inducer FT. *Science* 286: 1962-5
- Kaufmann K, Wellmer F, Muino JM, Ferrier T, Wuest SE, et al. 2010. Orchestration of floral initiation by APETALA1. *Science* 328: 85-9
- Khodashenas E, Varin L, 2010. Characterization of the function of AtST4c subfamily members in cytokinin-dependent growth control in Arabidopsis thaliana, master thesis, Concordia University
- Kiba T, Naitou T, Koizumi N, Yamashino T, Sakakibara H, Mizuno T. 2005. Combinatorial microarray analysis revealing arabidopsis genes implicated in

- cytokinin responses through the His->Asp Phosphorelay circuitry. *Plant Cell Physiol* 46: 339-55
- Klein M, Papenbrock J. 2004. The multi-protein family of Arabidopsis sulphotransferases and their relatives in other plant species. *J Exp Bot* 55: 1809-20
- Kobayashi Y, Kaya H, Goto K, Iwabuchi M, Araki T. 1999. A pair of related genes with antagonistic roles in mediating flowering signals. *Science* 286: 1960-2
- Kobayashi Y, Weigel D. 2007. Move on up, it's time for change--mobile signals controlling photoperiod-dependent flowering. *Genes Dev* 21: 2371-84
- Lee J, Lee I. 2010. Regulation and function of SOC1, a flowering pathway integrator. *J Exp Bot* 61: 2247-54
- Lee J, Oh M, Park H, Lee I. 2008. SOC1 translocated to the nucleus by interaction with AGL24 directly regulates leafy. *Plant J* 55: 832-43
- Li D, Liu C, Shen L, Wu Y, Chen H, et al. 2008. A repressor complex governs the integration of flowering signals in Arabidopsis. *Developmental cell* 15: 110-20
- Marsolais F, Boyd J, Paredes Y, Schinas AM, Garcia M, et al. 2007. Molecular and biochemical characterization of two brassinosteroid sulfotransferases from Arabidopsis, AtST4a (At2g14920) and AtST1 (At2g03760). *Planta* 225: 1233-44
- Mockler TC, Yu X, Shalitin D, Parikh D, Michael TP, et al. 2004. Regulation of flowering time in Arabidopsis by K homology domain proteins. *Proc Natl Acad Sci U S A* 101: 12759-64
- Moon J, Suh SS, Lee H, Choi KR, Hong CB, et al. 2003. The SOC1 MADS-box gene integrates vernalization and gibberellin signals for flowering in Arabidopsis. *Plant J* 35: 613-23

- Negishi M, Pedersen LG, Petrotchenko E, Shevtsov S, Gorokhov A, et al. 2001. Structure and function of sulfotransferases. *Arch Biochem Biophys* 390: 149-57
- Niehrs C, Beisswanger R, Huttner WB. 1994. Protein tyrosine sulfation, 1993--an update. *Chem Biol Interact* 92: 257-71
- Okamoto JK, Szeto W, Lotys-Prass C, Jofuku KD. 1997. Photo and hormonal control of meristem identity in the Arabidopsis flower mutants *apetala2* and *apetala1*. *Plant Cell* 9: 37-47
- Ossipow V, Laemmli UK, Schibler U. 1993. A simple method to renature DNA-binding proteins separated by SDS-polyacrylamide gel electrophoresis. *Nucleic acids research* 21: 6040-1
- Piotrowski M, Schemenewitz A, Lopukhina A, Muller A, Janowitz T, et al. 2004. Desulfoglucosinolate sulfotransferases from Arabidopsis thaliana catalyze the final step in the biosynthesis of the glucosinolate core structure. *J Biol Chem* 279: 50717-25
- Putterill J, Robson F, Lee K, Simon R, Coupland G. 1995. The CONSTANS gene of Arabidopsis promotes flowering and encodes a protein showing similarities to zinc finger transcription factors. *Cell* 80: 847-57
- Rouleau M, Marsolais F, Richard M, Nicolle L, Voigt B, et al. 1999. Inactivation of brassinosteroid biological activity by a salicylate-inducible steroid sulfotransferase from Brassica napus. *J Biol Chem* 274: 20925-30
- Samach A, Onouchi H, Gold SE, Ditta GS, Schwarz-Sommer Z, et al. 2000. Distinct roles of CONSTANS target genes in reproductive development of Arabidopsis. *Science* 288: 1613-6
- Searle I, He Y, Turck F, Vincent C, Fornara F, et al. 2006. The transcription factor FLC confers a flowering response to vernalization by repressing meristem

- competence and systemic signaling in Arabidopsis. *Genes Dev* 20: 898-912
- Srikanth A, Schmid M. 2011. Regulation of flowering time: all roads lead to Rome. *Cell Mol Life Sci* 68: 2013-37
- Torti S, Fornara F, Vincent C, Andres F, Nordstrom K, et al. 2012. Analysis of the Arabidopsis shoot meristem transcriptome during floral transition identifies distinct regulatory patterns and a leucine-rich repeat protein that promotes flowering. *Plant Cell* 24: 444-62
- Varin L, DeLuca V, Ibrahim RK, Brisson N. 1992. Molecular characterization of two plant flavonol sulfotransferases. *Proc Natl Acad Sci U S A* 89: 1286-90
- Weigel D, Alvarez J, Smyth DR, Yanofsky MF, Meyerowitz EM. 1992. LEAFY controls floral meristem identity in Arabidopsis. *Cell* 69: 843-59
- Weigel D, Nilsson O. 1995. A developmental switch sufficient for flower initiation in diverse plants. *Nature* 377: 495-500
- Werner T, Schmulling T. 2009. Cytokinin action in plant development. *Curr Opin Plant Biol* 12: 527-38
- Wigge PA, Kim MC, Jaeger KE, Busch W, Schmid M, et al. 2005. Integration of spatial and temporal information during floral induction in Arabidopsis. *Science* 309: 1056-9
- Yasuda S, Liu CC, Takahashi S, Suiko M, Chen L, et al. 2005. Identification of a novel estrogen-sulfating cytosolic SULT from zebrafish: molecular cloning, expression, characterization, and ontogeny study. *Biochemical and biophysical research communications* 330: 219-25
- Yoo SK, Chung KS, Kim J, Lee JH, Hong SM, et al. 2005. CONSTANS activates SUPPRESSOR OF OVEREXPRESSION OF CONSTANS 1 through FLOWERING LOCUS T to promote flowering in Arabidopsis. *Plant Physiol*

139: 770-8